Open Access

Journal of Energy and Power Technology

LIDSEN Publishing Inc.

Review

Ni-Silica-based Catalysts for CH_4 Reforming by CO_2 with Enhanced Stability: Recent Designs and the Impacts of Ni Confinement, Promoters, and Core-Shell Structures

Oscar Daoura [1, 2, *], Maya Boutros [1], Franck Launay [2]

1. Lebanese University, Laboratoire de Chimie Physique des Matériaux (LCPM/PR2N), Faculté des Sciences II, Campus Fanar, BP 90696 Jdeideh, Lebanon; E-Mails: oscardawra@hotmail.com; boutrosmaya@hotmail.com
2. Sorbonne Université, CNRS, Laboratoire de Réactivité de Surface, LRS, Campus Pierre et Marie Curie, F-75005 Paris, France; E-Mail: franck.launay@sorbonne-universite.fr

* **Correspondence:** Oscar Daoura; E-Mail: oscardawra@hotmail.com

Academic Editor: Zhao Yang Dong

Special Issue: Hydrogen Energy: Sustainable Production, Storage and Utilisation

Journal of Energy and Power Technology
2021, volume 3, issue 1
doi:10.21926/jept.2101006

Received: September 01, 2020
Accepted: December 31, 2020
Published: January 26, 2021

Abstract

CO_2 reforming of CH_4, also referred to as the Dry Reforming of Methane (DRM), is considered an excellent method to produce H_2 and CO (syngas), which are known to be used for the production of higher alkanes and oxygenates. Despite nickel's moderate toxicity, Ni-based heterogeneous catalysts are considered excellent candidates for use in DRM due to their reasonable performances and economic advantages. However, these materials also present severe drawbacks, such as sintering of the active phase and coke (carbon) deposition, which may, in certain cases, lead to severe catalyst deactivation. Several synthesis strategies, mostly based on the stabilization of nickel through oxide support, have been developed to overcome these issues. Silica-based materials are investigated widely due to their availability, high surface area, and the confinement capacity conferred by their controlled porosity. The present review summarizes the progress in the design of Ni/silica-

based catalysts for the dry reforming of methane between the years 2015 and 2018. The different strategies implemented are discussed to assist future research works in designing the anti-coking and anti-sintering nickel-silica-based catalysts.

Keywords
Ni-silica; CH_4 reforming; CO_2; Ni

1. Introduction

Given the abundance of methane (CH_4) and the diversity of its sources [1-3], along with its greenhouse gas character (second after carbon dioxide [4] but 25 times more specific [5]), the development of efficient strategies to take advantage of its energetic and chemical properties appears to be essential. Methane conversion is achieved through direct or indirect pathways. The direct pathway of combustion is the main approach followed to generate heat and electricity. However, the conversion of CH_4 through the indirect pathway of reforming processes, which produces syngas, which is further converted to valuable liquid and chemical intermediates, is also one of the possibilities considered [6]. Indeed, methane can react with the oxidants, such as H_2O, CO_2, and O_2, to produce syngas that is composed of dihydrogen and carbon monoxide in different molar ratios (Equation 1).

$$CH_4 + (H_2O \text{ or } CO_2 \text{ or } O_2) \rightarrow x\ H_2 + y\ CO \qquad \text{(Equation 1)}$$

Among the most important applications of syngas, the Fischer-Tropsch synthesis (FTS) reaction, which involves the conversion of CO and H_2 into valuable products, particularly alkanes, is of particular interest. However, FTS requires an H_2/CO reactant ratio of less than 1, and such a composition can neither be achieved directly through the partial oxidation of methane (H_2:CO = 2) nor through steam reforming (most often H_2:CO = 3); it can be achieved only after additional treatments, such as the use of selective membranes, which lead to additional costs and greater time consumption. Therefore, Dry Reforming of Methane (Equation 2, with CO_2), which produces the lowest H_2:CO ratio, appears to be a more convenient and direct approach. Besides the economic and energy benefits, DRM provides an important added advantage of environmental protection as it consumes another greenhouse gas, i.e., carbon dioxide [7-18].

$$CH_4 + CO_2 \rightarrow 2H_2 + 2CO \qquad \text{(Equation 2)}$$

Unfortunately, DRM is a highly endothermic reaction requiring high temperatures to reach the desired conversion levels. According to thermodynamic simulations, the maximal CH_4 conversion possible at 650 °C is approximately 80%, and a total conversion can be achieved only when the reaction temperature exceeds 800 °C [12, 16]. A major objective of the research works conducted on dry methane reforming is the development of stable catalysts that enable achieving high conversion rates at the mildest possible operating conditions and allow, under the stream, a constant selectivity in CO and H_2. However, syngas production is accompanied by side reactions, such as methane decomposition, the Boudouard reaction, and the Reverse Water Gas shift

reaction. The supporting noble metals, such as Rh, Ru, and Ir, are considered highly active, selective, and stable catalysts for DRM [19, 20]. However, due to economic concerns, the substitution of these noble metals with the less expensive and more abundant metals such as Ni that can demonstrate comparable catalytic activities is considered advantageous [21], even though Ni-based catalysts result in higher sintering and carbon deposition and also exhibit a certain level of toxicity [22].

The size of the metal particles, the physicochemical properties of the support, and the metal/support interaction are crucial parameters to be considered to optimize the stability of the catalysts. A wide number of oxides are used as supports, including SiO_2, La_2O_3, ZrO_2, TiO_2, CeO_2, Al_2O_3, and MgO [22]. Among these, SiO_2 has been investigated widely in terms of application in the preparation of nickel-based catalysts for the DRM reaction. Indeed, it is possible to prepare SiO_2 supports with high surface areas, tunable nanoscale pore structures/sizes, and variable accessible morphologies with the potential benefits of Ni dispersion and confinement. Moreover, it is supposed that the mechanism of the DRM reaction in the presence of SiO_2 support follows a mono-functional pathway, where both the reactants are activated by nickel alone [22]. This fact is crucial when studying the intrinsic activity of nickel. Although there are several published reviews on DRM [22-27], there is none that considers Ni-based-siliceous support catalysts specifically. In this context, the present bibliographic survey examines the current diversity of the Ni/SiO_2 catalysts. First, the advances in the Ni size control and confinement methods are discussed, following which different Ni-promoter combinations are explored. Next, the recent pathways used for the design of Ni/SiO_2 core-shell are highlighted while emphasizing their advantages and inconveniences. Particular focus is placed on the catalytic performance of these different systems evaluated according to the gas hourly space velocity (GHSV) used during their catalytic evaluation.

2. Ni Size Control/Confinement Strategies with Silica

In DRM, the use of small Ni nanoparticles is often preferred due to their known resistance toward coke deposition (Table 1, entries 1 and 2) [28, 29]. However, optimizing the size of these particles and keeping them relatively unchanged during the whole reaction is difficult.

Table 1 A selection of recent papers dealing with nickel size control and confinement within silica [28-48].

E	Year	Ni (wt.%)	NiO or (Ni^0) (nm)	Siliceous support	Preparation Method	Total flow (mL min^{-1})	GHSV L g^{-1} h^{-1}	Weight (mg)	T (°C)	Time (h)	CH_4 %	CO_2 %	Objectives	Ref
1	2017	7.5	(4.1)	SBA-15	IWI	30	22.5	80	700	50	79	85	Use of a chelating agent to incorporate smaller nanoparticle in the porosity	[28]
2	2017	5	(3.2)	SBA-15, MCM-41, KIT-6	WI, Griding	30	22.5	80	700	100	77	86	Preparation through solid grinding for better dispersion and smaller particles	[29]
3	2017	11	(11)	SBA-15, Al-MCM-41	WI with ethanol	100	150	40	750	23	91	94	Comparative study of micro and mesoporous materials	[30]
4	2017	10	27	SBA-15	IWI	60	24	150	750	4	90	92	Influence of operation conditions such as reaction temperature and gas feed	[31]
5	2015	4, 5, 10	3.8	M. SiO_2	IWI	60	72, 36, 16, 14.4	50	800	20	70	78	Effect of carbon chain number and amine concentration of Ni-aliphatic amine complex	[32]

6	2015	10	(8.2)	Mi. SiO_2	Electrospinning	80	48	100	700	5	58	77	Confinement of nickel inside nanofiber through electrospinning preparation	[33]
7	2017	2.5-15	(3.9)	HMS	OP	30	22.5	80	700	100	85	76	Development of active catalysts via simple route	[34]
8	2017	0.16-0.32	(2.6)	np SiO_2	Ni Deposition+ Si Coating	20	12	100	800	100	39	61	Particles size effect on the catalytic performances	[35]
9	2017	10	(5-9)	np SiO_2	Ultrasonic assisted I + Glucose	40	12	200	700	40	72	81	Promotion of the catalysts using pretreatments by CO_2, N_2 and H_2 before test	[36]
10	2017	5	3.3 (5)	SBA-15	TS	60	180	20	650	12	63	68	Influence of the calcination (rate and atmosphere)	[37]
11	2016	5, 10	4	np SiO_2	WI	60	144	25	600	12	6	n.d.	Influence of the pretreatment (reduction-oxidation-reduction)	[38]
12	2016	5	(2.5)	M. SiO_2	IWI	60	72	50	700	100	80	83	Hydrogen treatment before calcination	[39]
13	2016	10	6.6 (5.7)	SBA-15	Modified IWI	50	100	30	750	30	76	85	Ni-Hexamethylenetetramine as precursor for better confinement	[40]

14	2015	0.5-2	n.d.	SBA-15	IWI	n.d.	36	n.d.	600	50	60	n.d.	Ni_4O_4 cluster as Ni precursor for better incorporation and confinement	[41]
15	2015	5	(4.6)	M. SiO_2	IWI	60	72	50	700	16.6	70	72	Use of OAm/OAc organic pair toward anti-coking Ni/SiO_2	[42]
16	2017	7	4.2 (3.3)	SBA-15, SBA-15-TMB	Immobilization via poly(ethyleneimine) (PEI)	50	20	150	750	40	85	87	Confinement of Ni particles inside different pores sizes	[43]
17	2016	5	4.3 (8.5)	SBA-15	PVP assisted WI	62.5	75	50	750	25	80	88	PVP-assisted impregnation of nickel for better dispersion and confinement	[44]
18	2016	2.5-7.5	5	SBA-15, M. SiO_2	TS	88	52.8, 264	20, 100	500	12	69	63	Confinement of nickel using SBA-15	[45]
19	2018	10	5.7 (3.7)	SBA-15, M. SiO_2	IWI + ultrasound DP	80	240	20	750	35	60		Confinement of nickel inside the porosity of SBA-15 or SiO_2	[46]
20	2015	10	5	SBA-15	IWI and DP and RM	100	20	n.d.	850	24	65	88	Non-conventional impregnation method for better confinement and dispersion	[47]

21	2018	4.9	(2.3)	M. SiO_2 dendrites	OP		66.6	40	100	700	200	72	81	Encapsulation in dendritic mesoporous SiO_2	[48]

E: Entry; M.: Mesoporous; Mi.: Microporous; np: Non-Porous; TS: Two solvents; I.: Impregnation; IWI: Incipient wetness impregnation; WI: wet impregnation; DP: deposition-precipitation; OP: one-pot; RM: precipitation in presence of ascorbic acid; PVP: Polyvinylpyrrolidone; KIT: Korean Institute of Technology mesoporous siliceous support; HMS: Hollow mesoporous silica; n.d.: Not determined.

Examples of the studies concerning nickel and silica alone are presented in Table 1. The size control and stabilization of the nanoparticles are achieved mainly by confining the metal into the channels of porous silica supports (Figure 1). Various preparation methods are listed in Table 1 (entries 3-6) [30-33]. This strategy is quite promising as it protects the nanoparticles, particularly against the growth of carbon filaments [49, 50], without any decrease in their activity that might otherwise occur due to mass transfer limitation or due to coverage of the active sites as the nickel particles remain accessible to the reactants in the pores of the sample (Table 1, entry 7) [34].

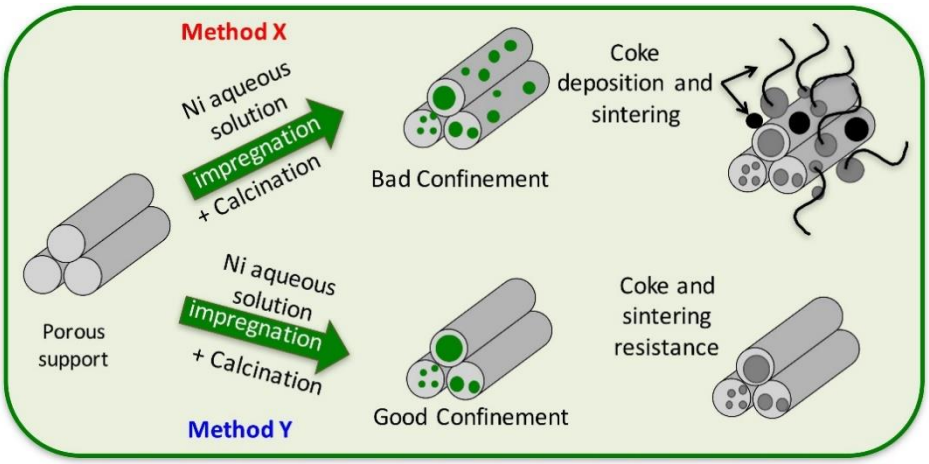

Figure 1 Illustration of the effect of nickel confinement in porous siliceous supports on nickel particle dispersion and DRM side reactions.

A few examples of efficient control of the particle properties using non-porous silica involve the dispersion of preformed Ni NPs (colloids) in such support (Table 1, entry 8) [35]. It is noteworthy that the modifications in the calcination step (heating rate, under air or inert gases, etc.) and certain pretreatments after the original preparation procedure (with H_2, N_2, CO_2, etc.) may also impact the nickel particle size and dispersion (Table 1, entries 9 to 12) [36-39].

2.1 Examples with Non-Porous Supports

Woo Han et al. (Table 1, entry 8) [35] prepared dispersions of Ni nanoparticles of highly uniform sizes centered on 2.6, 5.2, 9.0, and 17.3 nm, using a procedure that involved nickel acetylacetonate, trioctylphosphine, and oleylamine, and demonstrated that these colloids could be homogeneously deposited on non-porous silica spheres (400 nm) using ultrasonic-assisted wet impregnation. The obtained materials with Ni wt.% ranging between 0.16% and 0.32% were used in DRM at 800 °C to study the effect of the Ni NP size on the catalytic performances. The results revealed that the Ni nanoparticles of size 2.6 nm led to a 4-times higher turnover frequency for methane conversion compared to the NPs of size 17.3 nm (61.7 s^{-1} *vs.* 15.1 s^{-1}). The small Ni nanoparticles were definitely more advantageous in ensuring high activity and selectivity (39% and 65% of CH_4 and CO_2 conversion, respectively, with H_2/CO = 0.7 for 2.6 nm colloids *vs.* 15% and 22% and H_2/CO = 0.5 for the 17.3 nm ones) as long as their size was preserved. However, it is noteworthy that the Ni/silica catalysts reported by Woo Han et al. were evaluated under a rather low GHSV (12 L g^{-1} h^{-1}).

Non-porous siliceous supports were also utilized by Li et al. (Table 1, entry 9) [36], who demonstrated that Ni/C-SiO_2 (10 wt.%) catalysts prepared using an *in-situ* reduction impregnation method involving glucose solution were characterized (using XRD analysis) as having smaller and greatly dispersed NPs compared to those obtained using a traditional incipient impregnation method without glucose. However, the preparation procedure involving glucose initially led to poor catalytic performances due to carbon deposition associated with the use of an organic additive. Therefore, the authors had to use several pretreatments (during the preparation) to overcome such limitations. After optimization, the CO_2 pretreated catalyst was observed to exhibit higher coke deposition resistance due to the ability of CO_2 to eliminate carbon deposition under high temperature ($CO_2 + C \rightarrow 2CO$). However, the catalyst performances (70% conversion of CH_4 and CO_2 at 700 °C) were evaluated under quite low GHSV (12 L g^{-1} h^{-1}). In another study, Lovell et al. (Table 1, entry 11) [38] demonstrated that a reduction-oxidation-reduction (ROR) pretreatment (reduction followed by oxidation, and then re-reduction again) of calcined Ni-based solid might exert a significant impact on Ni-non-porous SiO_2 (Ni-SiO_2) catalysts prepared using an impregnation method involving Ni wt.% of 5 and 10. This pretreatment has been applied to different supported metals to generate small particles with high metal-support interaction. For instance, ROR method was used for the activation of cobalt catalysts used in the Fischer-Tropsch reaction [51]. After the ROR pretreatment, the Co species were re-dispersed, resulting in the formation of smaller Co deposits with stronger metal-support interaction. In other examples, the ROR pretreatment resulted in a reduction in the Ni deposit size for Ni-SiO_2 [52] or an increase in the dispersion of Ru in Ru-Co/Al_2O_3, which ultimately increased the CO conversion in the Fischer-Tropsch reaction [53]. In comparison to the samples that were just reduced without any pretreatment (R samples), Lovel et al (Table 1, entry 11) showed that the ROR pretreated samples were characterized by smaller and greatly dispersed Ni (12.8 nm for calcined *vs.* 8.7 nm for ROR pretreated 10 wt.% Ni-SiO_2). Using a rather important GHSV of 144 L g^{-1} h^{-1}, the authors revealed that after the ROR pretreatment, an enhancement occurred in the CH_4 conversion (from 57% to 68% at 800 °C), particularly for the solid containing 10 wt.% of Ni. Such improvement was attributed to the increased active metallic surface area caused by this type of pretreatment. However, the pretreatment did not lead to better stability in the 5 and 10 wt.% Ni-SiO_2 R and ROR samples (at 600 °C under GHSV of 144 L g^{-1} h^{-1}), with the particles exhibiting a dramatic decrease (≈ 30%) in activity after approximately 3-4 h of run time.

2.2 Examples with Porous Supports

Mesoporous supports provide a huge specific surface area, which facilitates metal dispersion. However, most of the available surface area has to be accessible to the metal precursors, which implies that dispersion strategies have to be implemented to take full advantage of these supports. Significant efforts have been put into utilizing original nickel precursors or the assistance of ligands or organic molecules. Certain authors also investigated the impact of support properties. The effects of the impregnation conditions have also been studied. Most of the works discussed in this section concern the materials obtained through the impregnation of preformed supports, although certain examples concerning one-pot strategies for Ni incorporation are presented as well.

2.2.1 Use of Original Nickel Precursors or the Assistance of Organic Molecules

One approach for controlling the size of the targeted Ni^0 NPs prepared using impregnation techniques is the use of specific nickel precursors. Li et al. prepared and utilized a hexamethylenetetramine (HMA) Ni(II) complex (referred to as $(NO_3)_2Ni(H_2O)_6(HMA)_2{\cdot}4H_2O$ by the authors), the formation of which could be attested using FTIR spectroscopy (Figure 2), to improve the insertion of Ni into mesoporous support of type SBA-15 (Table 1, entry 13) [40].

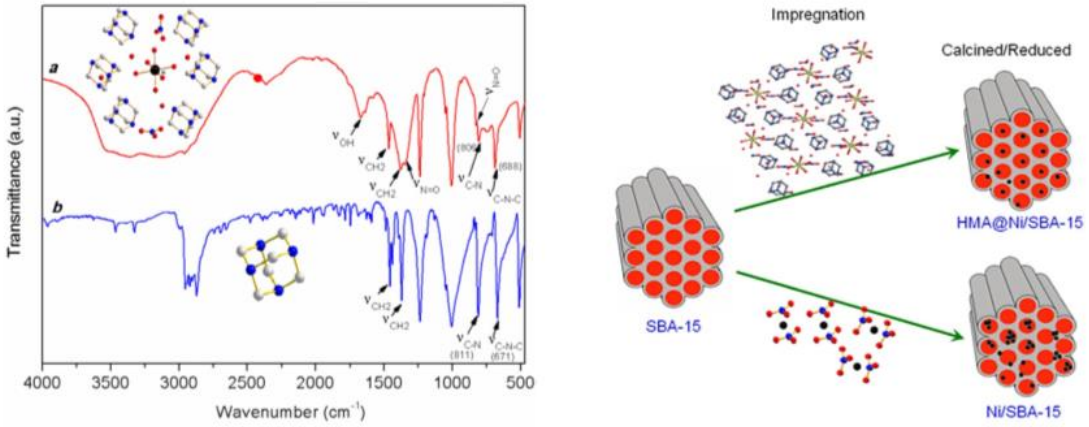

Figure 2 Left: The FTIR spectra of a: the *as*-synthesized $(NO_3)_2Ni(H_2O)_6(HMA)_2{\cdot}4H_2O$ complex and b: HMA; Right: The schematic illustration of the improved Ni dispersion for HMA@Ni/SBA-15 compared to Ni/SBA-15 [40].

HMA@Ni/SBA-15 (10.5 wt.% of Ni) was prepared through the incipient wetness impregnation of SBA-15 with the minimum amount of $(NO_3)_2Ni(H_2O)_6(HMA)_2{\cdot}4H_2O$ solution. For comparison, another material, Ni/SBA-15 (12.7 wt.% of Ni), was synthesized in a similar manner using a nickel nitrate aqueous solution. Smaller Ni NPs were observed for HMA@Ni/SBA-15 (4.9 nm) compared to Ni/SBA-15 (7.5 nm). Better incorporation of Ni, less porosity plugging, and higher dispersion were also deduced from the results of TEM analysis, N_2 physisorption analysis, and XRD measurements for HMA@Ni/SBA-15. Therefore, HMA@Ni/SBA-15 was a promising catalyst in good agreement with the characteristics of the materials used. At 750 °C, under a relatively high GHSV of 100 L g^{-1} h^{-1}, HMA@Ni/SBA-15 exhibited a considerably good stability during 30 h, with the CH_4 and CO_2 conversion rates of 76% and 85%, respectively. On the contrary, the CH_4 and CO_2 conversion rates achieved with Ni/SBA-15 derived from the nickel nitrate aqueous solution decreased from 71% and 77% to 65% and 68%, respectively.

In another study, the controlled formation of nickel oxide nanoparticles on SBA-15 was achieved through incipient wetness impregnation of the support using Ni_4O_4 cluster as the precursor (0.5 < Ni wt.% < 5) (Table 1, entry 14) [41] generating Ni_4/SBA-15. The use of such a ligand-stabilized cluster enabled the deposition of four Ni ions in close proximity on the silica support, which in turn, according to the authors, led to the formation of small and highly-dispersed NiO NPs after heat treatment. These clusters would exert a significant influence on the generation of NiO NPs compared to a conventional nickel(II) salt such as $Ni(OAc)_2$. The utilization of the cubane Ni_4O_4 precursor would result in, as the author hypothesized, a faster formation of small and highly-dispersed NiO nanoparticles, although the mean size and dispersion of the

particles were not reported. Undoubtedly, the resulting materials demonstrated enhanced stability toward DRM. Further precisely, at 550 °C, Ni_4/SBA-15 (1 wt.%) led to 23% CH_4 conversion even after 20 h, while a reference material Ni/SBA-15 containing 1 wt.% of Ni (1-Ni/SBA-15) was completely deactivated under similar conditions [41]. However, these results must be considered with a critical mindset as the DRM tests in both the evaluations were performed under a rather modest GHSV (36 L g^{-1} h^{-1}) compared to that used in work reported by Li et al. (Table 1, entry 13).

Organic additives may also be useful in this regard. Gao et al. (Table 1, entry 15) [42] prepared 5% Ni/SiO_2 catalysts promoted with oleylamine (OAm) and/or oleic acid (OAc) using an incipient wetness impregnation method. In this approach, OAm and/or OAc were used as surfactants, ligands, and/or reducing agents added on purpose to the solution of nickel nitrate prior to the impregnation in order to improve the dispersion of Ni on silica due to the strong interaction of the Ni precursors with OAm and OAc. Using a mixture of OAm and OAc with the spheres of mesoporous silica (particles size = 40-60 mm, specific surface area = 753 m^2 g^{-1}, mean pore size = 7.5 nm) produced, after calcination, small NiO particles in the Ni/SiO_2-OAmc material, and therefore, after reduction by H_2, to small Ni^0 NPs (Table 1, entries 5, 15) [32, 42]. Using this approach, the authors managed to achieve 5% Ni/silica with a nickel dispersion of *c.a.* 22% (mean diameter of the particles: 4.6 nm). The Ni dispersion was only 11.5% (8.8 nm particle diameter size) with OAc only (Ni/SiO_2-OAc). Accordingly, Ni/SiO_2-OAmc presented the highest conversion rate values in the series (CH_4: 73%, CO_2: 75%, with a rather good GHSV of 72 L g^{-1} h^{-1}) and the best stability (a decrease of 3%-5% after 17 h).

Zhang et al. evaluated certain other ligands, such as ethylenediamine (en) and citric acid (cit), which are known to be strong chelating agents, with aqueous $Ni(NO_3)_2.6H_2O$, to generate metal chelates prior to the impregnation of SBA-15 (7.5 wt.% of Ni) (Table 1, entry 1) [28]. The DRM catalysis tests with the corresponding materials revealed that ethylenediamine (en) and citric acid (cit) play a positive role in promoting the dry reforming of CH_4. Basically, the strong coordination ability of these ligands would inhibit the aggregation of the nickel species in the early stage of catalyst preparation, thereby contributing to the formation of well-dispersed Ni particles with low diameter size [below 6 nm for 7.5 wt.% Ni/SBA-15(en)] compared to the 18.9 nm diameter size of a reference Ni/SBA-15 prepared using a more conventional impregnation method [7.5 wt.% Ni/SBA-15(IWI)]. Again, the better dispersion obtained in the presence of chelating agents led to improved catalysis results [45% *vs.* 12% for CH_4 and 55% *vs.* 25% for CO_2 conversions at 600 °C for Ni/SBA-15(en) and Ni/SBA-15(IWI), respectively]. It is noteworthy that the GHSV used was more modest (22.5 L g^{-1} h^{-1}) compared to the one in the study by Gao et al. (72 L g^{-1} h^{-1}), who used oleylamine and oleic acid. However, Zhang et al. performed the stability test for a longer duration (50 h) without observing any significant decreases in the CH_4 and CO_2 conversion rates.

Furthermore, functionalized polymers are employed for improving the incorporation of Ni precursor without affecting the dispersion of the resulting Ni(0) particles. Polyethyleneimine (PEI), which is used as a stabilizer, reducing agent, and capping agent for the synthesis of nanoparticles in aqueous solutions [54, 55], was evaluated by Kang et al. (Table 1, entry 16) [43] for the introduction of nickel(II) within hexagonally-ordered mesoporous materials such as SBA-15 and the mesocellular foams such as SBA-15-TMB. PEI was first dissolved in deionized water and then contacted with $Ni(NO_3)_2.6H_2O$ to obtain PEI-Ni complexes prior to the impregnation of the supports up to 7 wt.% (inorganic weight percentage), producing PEI-Ni/SBA-15 and PEI-Ni/SBA-15-TMB, respectively. In the impregnation step, PEI-Ni complexes were expected to develop strong

interactions with the mesoporous silica. The best nickel incorporation was achieved for SBA-15-TMB, probably due to a better fit between the mean pore diameter and the PEI-Ni complexes. Both PEI-Ni/SBA-15 and PEI-Ni/SBA-15-TMB exhibited reasonable performances [*c.a.* 85% for CH_4 and CO_2 conversions] and acceptable stability. A decrease of only 5% to 8% was observed in the CH_4 and CO_2 conversion rates within 40 h. However, it is noteworthy that the authors used a rather low GHSV (20 L g^{-1} h^{-1}). In a parallel investigation, Yang et al. (Table 1, entry 17) [44] investigated the influence of poly(N-vinyl-2-pyrrolidone) (PVP), another nonionic polymer [56], on the Ni dispersion of the materials upon the wet impregnation of SBA-15 using $Ni(NO_3)_2.6H_2O$ as the nickel source. Here, similar to the previous examples, which involved PEI, PVP was used as a ligand of Ni^{2+} during its incorporation onto silica. In order to better understand the potential role of PVP, the authors varied the amounts used, for which they prepared a series of Ni/SBA15-PVP materials targeting 5 wt.% of Ni (PVP not included) with different nPVP/nNi molar ratios (1/X = 1/7500, 1/5000, 1/2000, 1/1000, 1/100, etc.) and one reference sample (Ni/SBA15, no PVP). The TEM, H_2 sorption, and XRD measurement results demonstrated that the 1/X ratio influenced the nickel confinement and dispersion. Therefore, the Ni/SBA15-PVP solids with 1/X = 1/5000, 1/2000, and 1/1000 presented the dispersion values of 12.5%, 11.8%, and 12.2%, respectively and small Ni^0 particles (8, 8.5, and 8.2 nm, respectively), while Ni/SBA15, Ni/SBA15-PVP (1/7500), and Ni/SBA15-PVP(1/100) presented larger aggregates and bigger particles on the external surface of the support. These characteristics were in agreement with the catalysis performances exhibited by the materials measured under a reasonable GHSV (75 L g^{-1} h^{-1}). Under these conditions, the Ni/SBA15-PVP solids with 1/5000, 1/2000, and 1/1000 ratios exhibited rather good stability at 750 °C after 25 h on stream, with almost no decrease in the CH_4 and the CO_2 conversions (stable at 80% for both), while with Ni/SBA15, Ni/SBA15-PVP (1/7500), and Ni/SBA15-PVP(1/100), the activity decreased by 15% after 25 h. A detailed study of the solids recovered at each step of catalyst preparation, i.e., at impregnation, drying, and calcination, generated results that were compatible with the formation of specific complexes of Ni by its coordination to the N and O atoms of PVP, which would reduce the redistribution of the metal, resulting in better dispersion and stabilization of the metal.

2.2.2 Impact of Supports and Impregnation Conditions

The silica support may itself play an important role in the control and confinement of nickel NPs. Certain works concerning the influence of the porosity of the supports (either micropores *vs.* mesopores or among mesopores with different sizes) on the nickel size and dispersion are discussed ahead.

In 2017, Drobna et al. (Table 1, entry 3) [30] reported a complete study that involved the use of zeolites such as MFI and FAU, Al_2O_3, mesoporous aluminosilica such as Al-MCM-41, or mesoporous silica such as SBA-15, coupled with Ni, to investigate the relationship between the catalysis performances and the textural properties of the supports. The Ni-based catalysts with 11 wt.% of Ni were prepared through wet impregnation in ethanol, although such a loading did not allow all the Ni NPs to be confined within the porosity even in the cases of Ni/SBA-15 and Ni/Al-MCM-41. Nevertheless, both Ni/SBA-15 and Ni/Al-MCM-41, with Ni particle sizes of 11 nm, exhibited the best performances in DRM (approximately 80% CH_4 conversion) after 20 h on stream under a GHSV of 150 L g^{-1} h^{-1}. In the case of Ni/MFI with the nickel particle size of 29 nm, the conversion

value was 55%, which appeared to be rather unusual with such size and under such harsh test conditions.

Similarly, Zhang et al. (Table 1, entry 2) [29] reported a study focusing on ordered mesoporous silica materials with either different pore diameters (Ni-SBA-15 *vs.* Ni-MCM-41) or different pore structures (hexagonal *vs.* cubic such as KIT-6) and used an original Ni incorporation method based on solid-state grinding. The materials with 5 wt.% of Ni were prepared from the mixtures of the support and the Ni source ($Ni(NO_3)_2.6H_2O$) without any significant degradation in the textural properties of the support compared to the reference ones obtained using conventional impregnation. The Ni particles on the Ni-SBA-15 samples prepared using this solid-state grinding method were among the smallest ones obtained in the study (compared to MCM-41 and KIT), implying that the nickel species were much more dispersed and in apparently greater interaction with the SBA-15 support, as a consequence of which, the Ni-SBA-15 sample exhibited the lowest decrease in activity (approximately 3% to 4% in general) in the DRM reaction after 100 h at 700 °C compared to 14%-15% decrease obtained for the Ni/SBA-15 sample prepared using an impregnation method. The catalytic activity and stability were observed to decline in the following sequence: Ni-SBA-15 > Ni-KIT-6 > Ni-MCM-41 > conventional Ni/SBA-15. However, the GHSV used in this work was relatively low (22.5 L g^{-1} h^{-1}). Therefore, Zhang et al. suggested that the solid-state grinding method improves the dispersion of the active component on carriers, although they did not report measuring the Ni dispersion.

Structured mesoporous materials provide high specific surface areas and high pore volumes that should facilitate high metal dispersions. However, the impregnation method used might be quite determining, as demonstrated in various previous studies. In the study reported by Kaydouh et al. (Table 1, entry 18) [45], who claimed to have prepared a series of Ni/SBA-15 catalysts with 2.5 < Ni wt.% < 7.5% with improved metal insertion into the pore structure, better confinement of the metal in comparison to that obtained using the conventional incipient wetness impregnation was achieved by using, for the first time, “Two-Solvents” (TS) impregnation. The innovation resided in the protocol, which involved: i) suspending the siliceous support in an apolar organic solvent (cyclohexane) and ii) adding a volume of an aqueous solution containing the adequate quantity of Ni precursor that was precisely equal to the pore volume of the support. Owing to the extremely low miscibility of water with the organic solvent, the aqueous solution containing the Ni precursor was supposed to penetrate the porosity more easily compared to its penetration in the absence of the organic co-solvent [57]. The success of the procedure was confirmed by the TEM and SEM results, particularly for the materials with 2.5 and 5 wt.% of Ni. The resulting catalysts reduced under H_2 at 650 °C and tested in DRM exhibited rather high activity and considerably good stability for 12 h (GHSV = 52.8 L g^{-1} h^{-1}).

Other approaches that have been implemented include the deposition-precipitation (DP) method, originally reported by Geus et al. [58]. Practically, the preparation of Ni/SiO_2 catalysts using the DP method involves the precipitation of the nickel species onto the silica surface via an increase in the pH of the Ni salt solution used for impregnation. Subsequently, Ni-anchoring occurred on the basis of the kinetic competition between two types of reactions, the Ni-O-Si heterocondensation/polymerization and the Ni-OH-Ni olation/polymerization, which lead to the formation and growth of nickel phyllosilicate and nickel hydroxide, respectively [59]. Rodriguez et al. (Table 1, entry 19) [46] prepared four materials with up to 10 wt.% of Ni impregnated onto SBA-15, and another mesoporous SiO_2 support using either the DP method (in the presence of

urea) or the incipient wetness impregnation (IWI) combined with ultrasound. The TEM images (Figure 3) depicted fibrous structures for SBA-15-DP and SiO_2-DP calcined samples, while no such observations were made when the IWI impregnation was used.

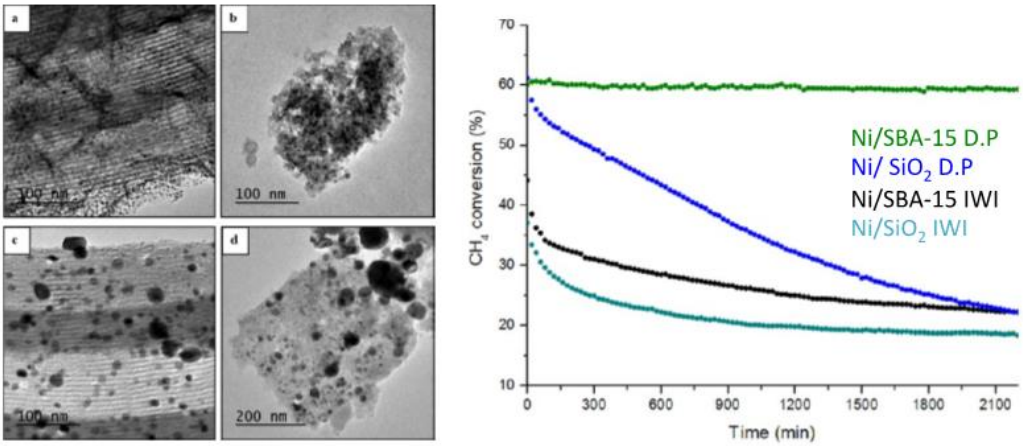

Figure 3 Left - TEM images of reduced: a: Ni/SBA-15 DP, b: Ni/SiO_2 DP, c: Ni/SBA-15 IWI, and d: Ni/SiO_2 IWI; Right - CH_4 conversion in the reaction of DRM at 750 °C under one of the best GHSV (240 L g^{-1} h^{-1}) reported [46].

According to the XRD, XANES, and EXAFS results, these observed structures corresponded to Ni phyllosilicates that are formed upon calcination of dried impregnated solid and, which, after reduction, produce small and well-dispersed Ni NPs (mean size of approximately 4.4 nm as confirmed by the particles size distribution measurement using TEM). The authors stated that the use of DP impregnation led to the confinement of the nickel particles at the inner surface of Ni/SBA-15, rendering them much more active (60% for CH_4 conversion) compared to those prepared using a conventional approach (35%-40%) and also more stable [no deactivation in the case of Ni/SBA-15-DP *vs.* a 20% deactivation in the other case (IWI)] (Figure 3). These results demonstrated that the confinement of nickel prevents sintering and coke deposition. Moreover, the GHSV value used in that work is one of the highest ones (240 L g^{-1} h^{-1}) reported in the literature.

Galvez et al. (Table 1, entry 20) [47] also attempted to evaluate the influence of the preparation method on the synthesis of 10 wt.% Ni/SBA-15. Three different synthesis methods were evaluated, *i.e.,* the incipient wetness impregnation (IWI), the deposition-precipitation (DP), and precipitation in the presence of ascorbic acid as a reducing agent (RM). In the last method, the catalyst was prepared following a procedure quite similar to the conventional DP method, except for the addition of ascorbic acid to the support suspended in distilled water after the introduction of urea. The authors of this work demonstrated that the physicochemical features of the obtained materials were influenced strongly by the preparation procedure used. The DP and RM methods led to the Ni particles being confined in the mesopores of SBA-15 (verified by TEM), while the simple IWI method led to the Ni particles being mostly deposited on the outer surface of the silica grains. The dispersion values of the Ni(0) phase obtained from the H_2 chemisorption experiments were observed to be enhanced for the DP (8.5%) and RM (8.7%) catalysts in comparison to the IWI catalyst (2.7%). Such differences were also reflected in the activity, selectivity, and stability exhibited in the DRM. After 24 h on stream, under a relatively modest GHSV (20 L g^{-1} h^{-1}), the

Ni/SBA-15-RM prepared using ascorbic acid produced a CH_4 conversion rate (65%) that was quite close to the conversion rate obtained with Ni/SBA-15-DP (67%) and significantly higher than the rate obtained in the presence of the solid prepared using the IWI method (40%) that underwent rapid deactivation. Therefore, the authors concluded that the addition of a reducing agent during the precipitation synthesis method led to the catalyst exhibiting improved stability, relatively higher activity, and enhanced selectivity toward DRM. It is, however, noteworthy that the dispersions of nickel on the solids prepared using the DP and RM methods were quite similar, although the TPR results revealed higher reduction temperatures in the case of the DP catalyst, which was attributed to better metal-support interactions. The authors concluded that the decrease in the textural properties upon Ni addition was due to the incorporation of Ni inside the pores. However, such decrease (approximately 65% and 50% of the specific surface area and the pore volume, respectively) can rather be explained by a certain level of degradation of SBA-15 due to the presence of urea, which when thermally decomposed, generates NH_3 that might be responsible for the alkaline attack of silica [59].

2.2.3 One-Pot Strategies for Ni Incorporation

One-pot (OP) incorporation of Ni is an alternative strategy that involves incorporating the nickel source directly into the silica's synthesis gel. This strategy could be promising in terms of simplicity and nickel dispersion throughout the resulting material. However, the one-pot preparation method is limited by the partial incorporation of the metal cation, particularly during the synthesis reactions performed under acidic conditions. Another strong limitation of this method when applied to mesoporous materials is associated with the decrease in the textural properties of the resulting samples. Indeed, when the metal salt is added directly into the synthesis gel, the structuration of the pores could be modified in comparison to the use of the silica precursor alone. For instance, while a decrease of approximately 20% could be achieved in the S_{BET} with the use of post-synthesis methods such as TS, IWI, etc. [45-47] for metal introduction, a worse deterioration (approximately 80%) is achieved with OP pathways [12, 17]. In this section, a few examples of the works concerning the successful preparation of Ni-based silica using the one-pot strategy are discussed.

Wang et al. (Table 1, entry 7) [34] evaluated the OP procedure with HMS mesoporous silica obtained using an S^0I^0 assembly pathway [60]. Four HMS samples (denoted as xNi-HMS) incorporating different Ni loadings (x = 2.5%, 5%, 7.5%, 10%, and 15%) were synthesized using dodecylamine as the structure-directing agent, followed by a comparison of these samples with Ni/HMS (7.5 wt.% of Ni) prepared through incipient wetness impregnation (IWI). The authors indicated different advantages of using the one-pot strategy with HMS. First, such a synthesis was considered time-saving and convenient in operation. Second, the xNi-HMS materials were prepared at room temperature without hydrothermal crystallization, which minimized energy consumption. Third, the template used for HMS was a primary amine, which is much less expensive compared to block polymers such as Pluronic 123 (used for SBA-15) and can be recovered through solvent extraction. Wang et al. reported that highly dispersed/confined small and homogeneous particles of Ni were observed in the xNi-HMS samples. However, the CO chemisorption results revealed that the dispersion range obtained for these solids was between 6.9% and 5.2%, which are not adequately high values. Moreover, the dispersions appeared to be

close to the one obtained with impregnated Ni/HMS (4.3%). The 2.5Ni-HMS exhibited the highest Ni dispersion (6.9%) and led to higher catalysis performances in DRM compared to its analogs with x = 5, 7.5, 10, and 15 wt.% of Ni as well as to the reference solid 7.5Ni/HMS. According to Wang et al., the solids obtained using this one-pot approach exhibited excellent stability, with approximately 90% of CH_4 and CO_2 conversion rates, respectively, at 800 °C, due to the strong anchoring effect of the silica wall that improved the resistance of the particles toward coking and sintering. However, it is noteworthy that these conversions were obtained under a rather low GHSV (22.5 L g^{-1} h^{-1}).

Tian and co-workers (Table 1, entry 21) [48] also used a one-pot synthesis to obtain Ni@SiO_2 catalyst for DRM, beginning with Ni nanoparticles encapsulated in dendritic silica structures. Ni@SiO_2 with 4.9 wt.% of Ni thus prepared exhibited a better dispersion of Ni with smaller nanoparticles (2-3 nm) compared to the reference material (4.8 Ni wt.% with 16 nm particles) obtained using a conventional impregnation method. In the latter, the Ni NPs were observed at both inner and outer surfaces, and the resulting solid underwent a total deactivation at 700 °C after 50 h on stream, while the material prepared using the one-pot synthesis exhibited high stability (81% and 72% for CO_2 and CH_4 conversions, respectively, after 50 h) although at a rather low GHSV value (40 L g^{-1} h^{-1}). Using theoretical calculation, the authors determined the formation energy of the different C clusters on the Ni particles, revealing that the growth of carbon nanotubes was difficult on the surface of small and confined nanoparticles obtained using the one-pot strategy.

3. Promoters and Bimetallic Ni-silica based Catalysts

Combining nickel with other metals or oxides may lead to synergistic effects as it would change the surface properties of Ni, thereby conferring better catalytic performances than exhibited when using Ni alone [26]. In this section, the contribution of the various additives that were used to promote nickel-silica based catalysts in the DRM reaction is presented (Table 2).

Table 2 A selection of papers dealing with promoters and bimetallic catalysts published between 2015-2018 [45, 61-92].

E	Year	Ni (wt.%)	NiO or (Ni^0) (nm)	Promoters element	Siliceous support	Preparation method	Total flow (mL min^{-1})	GHSV L g^{-1} h^{-1}	Weight (mg)	T (°C)	Time (h)	CH_4 %	CO_2 %	Objectives	Ref
1	2017	0-10	(5.7)	Co (0-10 wt.%)	SiO_2 from phyllosilicates	HM	30	60	30	750	100	86	89	Ni-Co alloy derived from phyllosilicates	[61]
2	2018	2.5-10	n.d.	Co (0-10 wt.%)	SBA-15	Co-P	60	72	50	700	50	70	60	Bimetallic Ni-Co for higher activity and stability	[62]
3	2017	4-5	n.d.	Co (5 wt.%)	Spherical M.SiO_2	IWI	60	72	50	700	30	79	82	OAm/OAc organic pair for the improvement of performances of Ni-Co bimetallic catalysts	[63]
4	2018	2.5-5	16.9	Co (1-5 wt.%)	SBA-15	WI	60	36	100	750	4	80	90	Ni/SBA-15 promoted by Co	[64]
5	2015	20.9	(8)	Cu (0-16 wt.%)	Spherical np SiO_2	HM	20	13.3	90	700	30	71	n.d.	Hierarchical Ni and Ni-Cu/SiO_2 derived from phyllosilicates (nanoparticles embedded in nanosheets)	[65]
6	2016	2.5-7.5	5	Ce (6 wt.%)	SBA-15, M. SiO_2	TS	88	52.8, 264	20, 100	500	12	69	63	Confinement of nickel using SBA-15	[45]
7	2017	10	5.3	Ce, Zr (CeZr both 57-84	np SiO_2	WI	60	144	25	700	24	50	n.d.	Examination of the intricate relationship between support	[66]

				wt.%)									structure and catalytic performances	
8	2017	5-7	(6.2)	Ce (2.5 wt.%)	M. SiO_2	In situ particles preparation	30	12	150	750	40	83	95	In-situ preparation of Ni nanoparticles in nanochannels of cerium-modified silica aerogels [67]
9	2016	10	(18)	Ce (4.4 wt.%)	M. SiO_2	n.d.	30	12	150	750	40	89	97	Design of NiCe@m-SiO_2 core-shell structure for better confinement [68]
10	2016	10	(16.3)	Ce (0-20 wt.%)	Illite clay (mainly containing SiO_2)	Co-I	100	60	100	800	4	88	73	Illite clay as support for promoted Ni by Ce [69]
11	2015	10	9	Ce, Zr (both CeZr 10 wt.%)	SBA-15	IWI and P	100	20	n.d.	n.d.	n.d.	n.d.	n.d.	Non conventional impregnation method for better confinement and dispersion [70]
12	2015	10	(2.3)	Ce (3 wt.%)	M. SiO_2 nanospheres	IWI	30	12	150	750	20	90	95	Immobilizing Ni in the porosity of mesoporous SiO_2 and preparation of modified Ce-SiO_2 support [71]
13	2015	5	5	Ce (6 wt.%)	SBA-15	TS and Co-I	n.d.	264	20	n.d.	n.d.	n.d.	n.d.	Order of Ni and Ce addition on the catalytic performances [72]
14	2107	17.5	9.7 (8.4)	La (1-7 wt.%)	M. SiO_2	OP	n.d.	72	50	700	40	72	74	Facile one-pot preparation of Ni-La_2O_3/SiO_2 [73]

15	2017	1	2-3	La (0.2-34 wt.%)	np SiO_2	IWI	n.d.	n.d.	n.d.	500	43	n.d.	n.d.	Study the improvement of La doping	[74]
16	2016	5	2.5	La (0-5 wt.%)	SBA-15	Modified IWI	60	72	50	700	12	83	87	Promotional effect of La	[75]
17	2016	10	19	La (3 wt.%)	SBA-15	IWI and Co-I	60	24	150	750	24	92	95	Influence of Lanthanide promoters on Ni/SBA-15	[76]
18	2018	12	n.d.	La (n.d.)	M. SiO_2	Stöber	30	18	100	800	8	81	84	$LaNiO_3$ nanocube used as Ni precursor embedded in mesoporous SiO_2	[77]
19	2017	10	10	Sm, Y, Zr (3 wt.%)	SBA-15	TS	40	12	200	700	5	71	75	Comparative study of samaria, yttria and zirconia as promoters for Ni/SBA-15	[78]
20	2017	10	7.2	Sm (0.5-1.5 wt.%)	SBA-15	TS	40	12	200	700	5	54	64	Sm promotional effect on Ni and Co based catalysts	[79]
21	2017	10	7	Sm (0.5-3 wt.%)	SBA-15	TS	40	12	200	700	11.5	73	75	Promotional effect of samarium for better dispersion	[80]
22	2018	2.5-10	n.d.	Ti (5-18 wt.%)	SBA-15	WI	n.d.	1.5	50	700	12	66	71	Promotional effect of titanium nitride (due to its thermal stability)	[81]
23	2016	3, 5, 10	n.d.	Gd (0.2 wt.%)	M. ZSM-5	WI	33, 166	10, 50	200	750	100	93	n.d.	Effect of Gadolinium on the stabilization of Nickel/ZSM-5	[82]
24	2015	10	n.d.	Fe_2O_3 (n.d.)	Mi. SiO_2	OP	90	54	100	800	1	66	93	Nickel ferrite supported catalysts (effect of dispersion)	[83]

25	2018	5	n.d.	Sc (0-3 wt.%)	MCM-41	Co-I	65	39/78	100/50	800	7	85	90	Promotional effect of scandium	[84]
26	2017	5	(4)	Boron nitride (n.d.)	M. SiO_2	I in sonic bath followed by rotary evaporation	30	15	120	n.d.	100	89	n.d.	Synthesis of stable structure of well confined Ni@mesoporous SiO_2 supported on hexagonal boron nitride	[85]
27	2016	n.d.	n.d.	Zr (n.d.)	SiO_2	WI	60	14.4	250	n.d.	n.d.	n.d.	n.d.	Low temperature reforming using Zr-promoted Ni/SiO_2	[86]
28	2018	3	(8.6)	In (2 wt.%)	np SiO_2	DP	20	40	30	675	24	31	69	Reducing the coke formation by adding Indium (Ni-In/SiO_2)	[87]
29	2017	n.d.	(4)	Zr, Mn (n.d.)	np SiO_2	Co.I	60	14.4	250	n.d.	n.d.	n.d.	n.d.	Influence of reduction temperature on the performances of catalysts	[88]
30	2015	n.d.	n.d.	Mn, Zr (n.d.)	np SiO_2	WI	60	20	n.d.	800	60	75	n.d.	Promotional effect of both Mn and Zr in the same time	[89]
31	2015	n.d.	n.d.	Mn (n.d.)	np SiO_2	Sol-Gel + P	30	90	20	750	50	16	30	Promotional effect of Mn	[90]
32	2017	9	n.d.	Ca (0-9 wt.%)	MCF's zeolite	Sol-Gel and WI	60	24	150	750	75	91	99	Effect of CaO on the stabilization towards coking	[91]
33	2018	18-27	(6.6)	Mg (0-11 wt.%)	Hollow Hierarchical SiO_2	Hydrothermal-P	18	30	100	700	50	89	92	Promotional effect of MgO	[92]

E: Entry; M.: Mesoporous; np: Non-Porous; TS: Two solvents; I.: Impregnation; IWI: Incipient wetness impregnation; WI: wet impregnation; Co-P: Co-precipitation; DP: deposition-precipitation; OP: one-pot; P: precipitation; HM: hydrothermal method; n.d.: Not determined; OAc: Oleic acid; OAm: Oleylamine

Metals, such as Pt, Ru, and Ir, have been well-recognized as DRM catalysts for decades, demonstrating higher activity and better resistance to carbon compared to Ni [93-97]. When associated with Ni, a small amount of noble metal usually assists in promoting the reducibility of nickel due to the higher affinity of the noble metal toward H_2 and the increase in the number of active sites [98-107, 108]. For instance, when Pt is added to nickel-based catalysts, a significant decrease in the barrier energy of CO_2 dissociation was observed [109, 110].

In the literature between 2015 and 2018, not many examples concerning the use of noble metals as promoters for Ni-silica based catalysts are available. Other metals, such as Co, Mg, Cu, and In, are preferred for DRM application. The combination of Ni and Co, for example, has been studied extensively. Bian et al. (Table 2, entry 1) [61] and Xin et al. (Table 2, entry 2) [62] separately demonstrated that the Ni/Co ratio, in a Ni-Co alloy, is crucial for the catalytic performances of the resulting Ni-Co-silica catalysts. It was reported that 7Ni3Co exhibits high and stable activity, while 5Ni5Co, 3Ni7Co, and 10Co exhibit severe deactivation (e.g., CH_4 conversion after 30 h on stream decreased from 60% to 40% in the case of 10% Ni/SBA-15, while it remained stable (65%) for 50 h in the presence of Co [62]). Gao et al. (Table 2, entry 3) [63] observed small shifts in the binding energy values in the XPS (increase for Co and decrease for Ni compared to isolated Co and Ni, respectively), and emphasized the existence of an electron transfer from Co to Ni when both are combined, thereby revealing an intimate interaction between the two [111, 112]. According to the authors, the higher electron density in Ni would improve the metal-support interaction and protect Ni from sintering during the DRM reaction (Table 2, entry 4) [64, 113-115]. In addition, the better affinity of Co toward the oxygen species leads to an excellent coke resistance, resulting in a catalyst with higher stability and reactivity (Table 2, entries 2 and 4) [62, 64].

Wu et al. (Table 2, entry 5) [65] proposed Cu-Ni alloy nanoparticles species supported on silica nanosheets using a phyllosilicate intermediate, prepared using nickel and copper nitrate salts. Such a preparation method resulted in much higher metal-support interaction compared to the conventional impregnation methods, thereby producing finely-divided Cu-Ni nanoparticles with an average diameter of *ca*. 7 nm. However, the $CuNi_3/SiO_2$ catalyst [containing 5.5 wt.% and 20.9 wt.% of Cu and Ni, respectively] led to a slightly higher CH_4 conversion (72%) compared to that observed for Ni/SiO_2 [20.9 wt.% of nickel (66%)]. Indeed, the activation energy for CH_4 conversion derived from the slope of Arrhenius plots (logarithms of the conversion rates *vs.* 1/T at a temperature range of 500-700 °C) was similar for Ni and $CuNi_x$, when x was larger than 3. On the other hand, there was a significant impact on the stability and the minimization of carbon whisker formation after 30 h on stream at 700 °C, although this was achieved using a relatively low GHSV (13.3 L g^{-1} h^{-1}). The authors explained that Cu would assist in promoting the sintering resistance of the alloy nanoparticles, although for Cu-overdosed materials, the activation energy for CH_4 conversion was apparently higher.

Various other elements or their oxides/nitrides have also been investigated previously as promoters to improve the stability of nickel-based catalysts toward coke deposition, such as Ce (Table 2, entries 6-13) [45, 66-72], La (Table 2, entries 14-18) [73-77], Sm (Table 2, entries 19-21) [78-80], Titanium nitride [81], Gadolinium [82], Ferrite [83], Sc [84], and boron nitride [85], (Table 2, entries 22-26), *etc.* In a study, Yao et al. [86] (Table 2, entry 27) studied Ni-Zr-silica catalysts prepared through impregnation of the SiO_2 support with an aqueous solution containing $Ni(NO_3)_2$ and $Zr(NO_3)_4$ and demonstrated that such materials were catalytically more active in the DRM

reaction at low temperatures compared to their non-promoted counterpart Ni/SiO_2. Such a behavior could be related to the high activation ability of the Ni-Zr/SiO_2 materials for both CH_4 and CO_2. Therefore, the activation energy values obtained with Ni-Zr/SiO_2 were much lower than those obtained with Ni/SiO_2 [30.0 (CH_4) and 21.9 (CO_2) kJ mol^{-1} *vs.* 473.9 (CH_4) and 704.6 (CO_2) kJ mol^{-1}, respectively]. According to Yao et al., Zr-promoted catalysts would facilitate the activation of the CH bond in CH_4 and activate CO_2 by forming significant proportions of carbonates (Table 2, entry 27) [86]. In addition, the Ni-Zr/SiO_2 catalysts exhibited CH_4 and CO_2 conversions of only 4.5% and 9.1%, respectively, at 450 °C. Unfortunately, these authors did not work under high GHSV values (only 14.4 L g^{-1} h^{-1}). Károlyi et al. (Table 2, entry 28) [87] combined Ni with Indium (In) on SiO_2 support using a deposition-precipitation method, which involved the mixing of the Ni and the In precursors. The presence of 2 wt.% of In on the surface of 3 wt.% Ni/SiO_2 prevented coke formation in the DRM at 675 °C for 24 h under an acceptable GHSV of 40 L g^{-1} h^{-1}, as evidenced by the TPO curves of the spent catalysts. The improved stability exhibited by Ni-In/SiO_2 compared to Ni/SiO_2 was also related, as stated by the authors, to a change in the nickel adsorption properties [and its electronic structure] when indium was used as the promoter.

Oxides, such as MnO_x (Table 2, entries 29-31) [88-90], CaO, MgO, Y_2O_3, and Sm_2O_3, have also been evaluated for improving the performances of Ni catalysts. For instance, Amin et al. (Table 2, entry 32) [91] concluded that the introduction of CaO to Ni-based mesocellular silica foams using a sol-gel method renders the obtained catalyst more stable toward the DRM limitations. Similarly, MgO-promoted Ni/SiO_2 was evaluated by Zhang et al. (Table 2, entry 33) [92], who demonstrated that the uniformly-dispersed MgO basic promoter resulted in an increased CO_2-adsorbing affinity. Moreover, the formation of Mg-phyllosilicate induced CO_2 activation by the support, thereby improving the catalytic activity and coking resistance of the resulting material.

In another study, Taherian et al. (Table 2, entry 19) [78] compared the effect of three oxides (3 wt.%) on a 10 wt.% Ni/SBA-15 catalyst. The authors used zirconia (ZrO_2), yttria (Y_2O_3), and samaria (Sm_2O_3), and the precursors of these were added using the "two-solvent" method. The activity tests, which used a rather low GHSV (12 L g^{-1} h^{-1}) and the TPO revealed that the incorporation of samaria i) improved the metal-support interaction and the dispersion of Ni, leading to high methane conversion (approximately 75%) and ii) decreased the coke formation. The addition of yttria increased the CH_4 conversion, although it also enhanced the coke formation, unfortunately. Several other oxides of rare earth elements have been used in association with silica. Oemar et al. (Table 2, entry 16) [75] added La_2O_3 onto Ni/SBA-15 and demonstrated that the quantity of oxide has to be adjusted. Only a small amount of La (approximately 1 wt.%) was necessary to obtain the best catalytic performances [83% of CH_4 conversion at 700 °C for 10 h under a reasonable GHSV (72 L g^{-1} h^{-1})]. The 1% La-promoted Ni/SBA-15 material was much more active and stable compared to the un-promoted one. These authors concluded that in the presence of La, the highly-dispersed Ni catalyst was very active in the decomposition of CH_4, resulting in higher CH_4 conversion. In addition, the La oxide also actively adsorbs CO_2 and would assist in the removal of the deposited carbon on the catalyst surface, resulting in high catalytic stability. In addition, the presence of La was demonstrated to strongly inhibit the RWGS reaction (Table 2, entry 14) [73].

Ce has also been often employed as a promoter for the Ni-silica based catalysts. The synthesis of such catalysts is performed, for example, by using natural illite clay, which is a low-cost precursor (Table 2, entry 10) [69], or, more often, by beginning with non-natural silica supports. Irrespective of the structure (mesoporous, core-shell, or aerogels), the incorporation of Ce in the

catalyst formulation improved its performance in the DRM reaction (Table 2, entries 6-13) [45, 66-72]. Ce introduction also conferred self-decoking properties and favored the formation of small highly-dispersed Ni particles and the strengthening of the interaction between the metal and the support (Table 2, entries 8-13) [67-72]. It is noteworthy that more complex catalyst formulations, such as the combination of Ce and Zr, were considered to synthesize a silica/ceria-zirconia support for Ni deposition (Table 2, entry 7) [66]. Another rare-earth element, gadolinium has been tested successfully for the promotion of Ni/ZSM-5 in DRM (Table 2, entry 23) [82]. Sarkar et al. reported the formation of GdNi5 alloy with a particle size of 2-10 nm. In this case, the strong interaction and charge transfer from Gd to Ni, as evidenced by the XPS results, explained the low carbon deposition and the sintering of Ni.

4. Ni@silica Core-Shell Nanoparticles

One possible physical protection to prevent carbon deposition and efficiently inhibit the sintering of the metal (Table 3, entry 1) [116] is to cover the metal particles with at least one microporous oxide material that allows the access of the DRM reactants. This approach was tested with various materials, ranging from core-shell structures involving silica particles to porous materials that incorporate, into their walls, the metal introduced during the synthesis of the silica support (Figure 4). The latter has already been described in Section 2.2.3 and will not be discussed below.

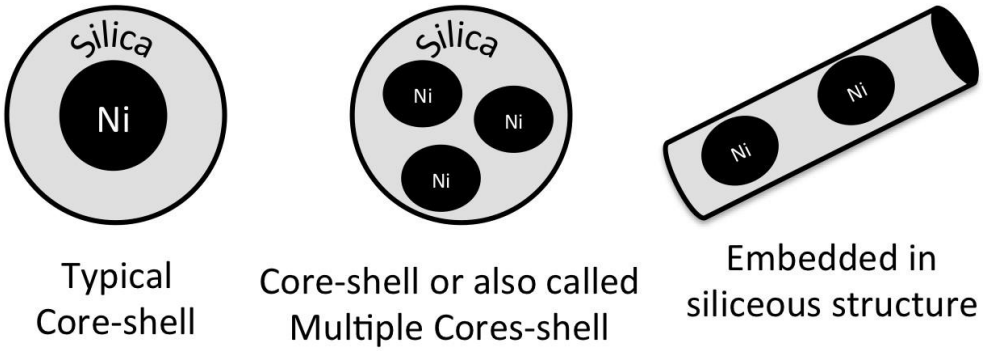

Figure 4 Different approaches leading to the physical protection of nickel by porous silica.

Table 3 A selection of papers dealing with core-shell catalysts published between 2015-2018 [66, 68, 71, 116-122].

E	Year	Ni (wt.%)	NiO or (Ni^0) (nm)	Promoters element	Siliceous support	Preparation method	Total flow (mL min^{-1})	GHSV L $g^{-1}h^{-1}$	Weight (mg)	T (°C)	Time (h)	CH_4 %	CO_2 %	Objectives	Ref
1	2016	11.6, 18.8	(8.5)	Mg (5.1, 9.2 wt.%)	M. SiO_2	HM	30	60	30	750	72	85	88	Ni-Mg phyllosilicates @silica used as catalyst	[116]
2	2017	10	5.3	Ce, Zr (CeZr both 57-84 wt.%)	np SiO_2	WI	60	144	25	700	24	50	n.d.	Examination of the intricate relationship between support structure and catalytic performances	[66]
3	2016	10	(18)	Ce (4.3 wt.%)	M. SiO_2	n.d.	30	12	150	750	40	89	97	Design of NiCe@m-SiO_2 core-shell structure for better confinement	[68]
4	2015	10	(2.3)	Ce (3 wt.%)	M. SiO_2 nanospheres	IWI	30	12	150	750	20	90	95	Immobilizing Ni in the porosity of SiO_2 mesopores and preparation of modified Ce-SiO_2 support	[71]
5	2015	29	10	No	Mi. and M. SiO_2	NiO suspended in CTABr then coated	40	48	50	750	25	54	66	Preparation of core-shell structure for better stability	[117]

					by SiO_2									
6	2017	5	(4.3)	No	Mi. SiO_2	OP	15	18	50	800	100	88	89	One-pot core-shell structure for better confinement	[118]
7	2018	10	(5-6)	No	silica nano-capsule	Reverse micelle approach	80	48	100	700	325	75	80	Siliceous nanocapsule for the confinement of nickel	[119]
8	2018	3-7	(4)	No	np SiO_2	OP	30	60	30	800	23	45	55	Sandwich-Like Silica@Ni@Silica Multicore-ShellCatalyst: Confinement effect against coke deposition	[120]
9	2018	25	(5-8)	No	SiO_2 nanotubes	HM	n.d.	36	n.d.	700	70	81	78	Confinement of Ni particles in silica nanotubes	[121]
10	2017	2.6-2.8	(7-9)	No	np SiO_2	IWI	n.d.	5	800	800	500	90	89	Core-shell structure using thin-felt microfibrous-structured $Ni@SiO_2/Al_2O_3/FeCrAl$ fabricated by one-step	[122]

E: Entry; M.: Mesoporous; Ma: Macroporous; np: Non-Porous; Mi: Microporous; IWI: Incipient wetness impregnation; WI: wet impregnation; OP: one-pot; HM: hydrothermal method; n.d.: Not determined.

Core-Shell Nanoparticles (CSNs) are a class of nanostructured materials that have been receiving increasing attention recently due to their important roles in various catalytic processes [123]. As discussed earlier, promoters are often added to the catalyst formulation to improve the performance of Ni in the DRM reaction. This strategy has also been considered in the approaches involving Ni/silica core-shell particles. The available examples in the literature deal with Ce (Table 3, entries 2-4) [66, 68, 71], Zr (Table 3, entry 2) [66], and Mg (Table 3, entry 1) [116]. The following paragraph presents a few examples of core-shell systems with varying scales of complexity. In all the cases, the ordered porosity of silica is generated using organic structure-directing agents that are later removed through calcination.

In a quite interesting work reported by Zhang et al. (Table 3, entry 5) [117], core-shell $NiO@SiO_2$ nanoparticles were prepared from the commercially available NiO NPs (10-20 nm) added to a silica precursor dispersed in a cetyltrimethylammonium bromide solution to construct a mesoporous silica framework around the NiO NPs, thereby preventing the formation of carbon species on their surface. The mesopores were generated after removing the surfactant molecules through calcination. As expected, the shell of silica suppressed the sintering of Ni and the growth of carbon filaments, while the mesopore channels allowed the reactants to diffuse with no limitation toward the surface of Ni, which could also be encouraging for other reactions such as CO_2 methanation. In DRM, coke deposition was demonstrated to be negligible after 39 h on stream at 850 °C under an acceptable GHSV (40 L g^{-1} h^{-1}), while the catalyst was relatively stable for 24.5 h. In addition, it was demonstrated that the catalytic performance of $Ni@SiO_2$ materials could be further improved by optimizing the microstructure of the core-shell nanoparticles and the surface of the Ni NPs inside the shell. Promotion with cerium was evaluated, for example, with the NiCe@m-SiO_2 catalyst containing 10.6 wt.% of Ni and 4.3 wt.% of Ce (Table 3, entry 3) [68]. The material was prepared through the hydrolysis and condensation of silica precursors added to a reverse microemulsion obtained by dispersing aqueous $Ce(NO_3)_3.6H_2O$ and $Ni(NO_3)_2$ in a mixture of cetyltrimethylammonium bromide, 1-butanol, and cyclohexane. NiCe@m-SiO_2 with nickel particle size ranging between 14 and 24 nm was tested for 40 h at 750 °C, and it proved to be a better catalyst (90% CH_4 conversion) compared to $NiCe/SiO_2$ prepared through the impregnation of silica (75% of CH_4 conversion). However, the GHSV value (12 L g^{-1} h^{-1}) used in the study was quite low.

Multiple-cores@shell catalysts comprising multiple Ni nanoparticles as the core and microporous silica as the shell (M-$Ni@SiO_2$) may also be synthesized using a one-pot reverse-phase microemulsion strategy. As an example, in the work of Peng et al. (Table 3, entry 6) [118], the M-$Ni@SiO_2$ material containing 5 wt.% of nickel was prepared by introducing concentrated ammonia and tetraethoxysilane into a reverse microemulsion prepared by dispersing an aqueous Ni^{2+} solution in a mixture of polyethylene glycolmono-4-nonylphenyl ether (NP-5) and cyclohexane. Following two days of hydrothermal treatment, the particles were destabilized using ethanol and then collected through centrifugation at 10000 rpm, followed by calcination at 800 °C and vacuum drying. In the freshly calcined Multiple-$NiO@SiO_2$ samples, the particle size of the ultra-fine Ni cores was approximately 4.3 nm, while the total average size of the core-shell particle was 30 nm and the pore size of the microporous shell was 1.5 nm. Peng et al. demonstrated that after *in situ* reduction, M-$Ni@SiO_2$ exhibits good catalytic activity and stability (90% and 92% for CH_4 and CO_2 conversions, respectively, after 100 h). No carbon species could be detected in TGA-DSC after 100 h of DRM at 800 °C, although the GHSV worked with was quite low (18 L g^{-1} h^{-1}) (Figure 5). M-

Ni@SiO_2 led to a CH_4 conversion quite similar to that of Ni/SiO_2 prepared using a conventional impregnation method and that of the commercial Ni/Al_2O_3. However, Ni/SiO_2 and Ni/Al_2O_3 presented more coke deposition, as revealed in the TGA characterization of the spent catalysts. In the case of M-Ni@SiO_2, all the Ni particles were confined in the microporous silica shell, which led to a lack of physical space for the growth of carbon species, particularly the filamentous and encapsulating carbon. However, it is noteworthy that the comparison was not really fair as the Ni particles in M-Ni@SiO_2 were smaller than those in the other catalysts, which could also have contributed to the superior carbon resistance ability of the core-shell catalyst.

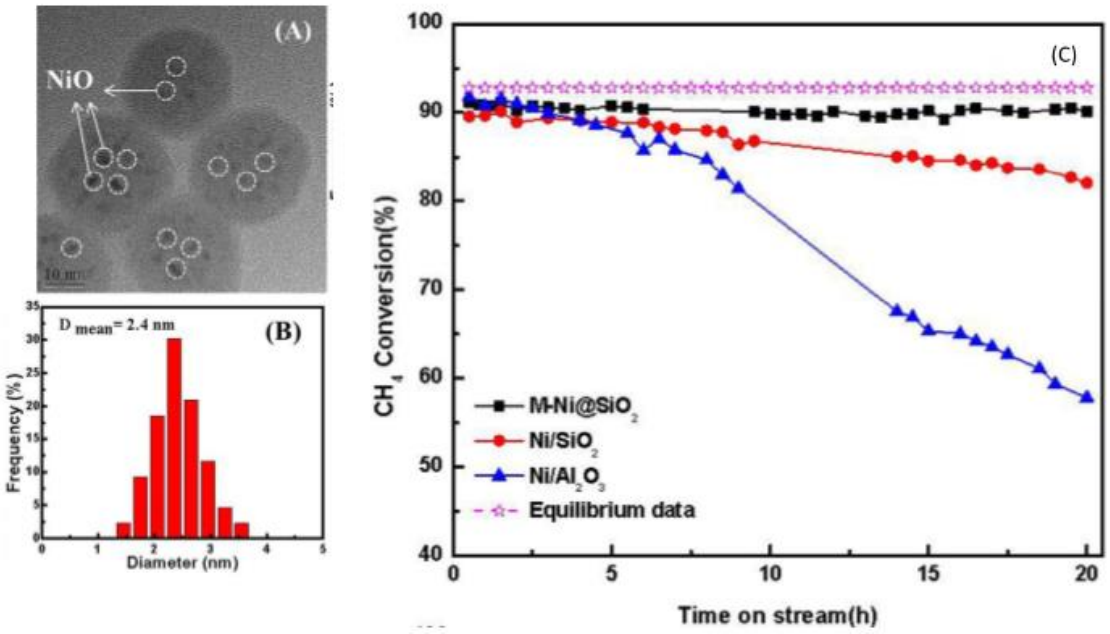

Figure 5 A and B: TEM and Ni particle size distribution of M-Ni@SiO_2 and C: comparison of the stability of different Ni-based silica or alumina catalysts toward the CH_4 conversion [118].

Further sophisticated objects have also been designed, such as hollow silica capsules, including Ni nanoparticles (work of Wang et al.) (Table 3, entry 7) [119]) or the sandwich-like Silica@Ni@Silica Multicore-shell systems (Table 3, entry 8) [120]. The latter were synthesized by Bian et al. using a four-step approach, in which SiO_2 nanospheres were prepared first, which were then covered by Ni phyllosilicates (PS) that were further protected by a silica shell and reduced under H_2. In a similar approach, Z. Li et al. (Table 3, entry 9) [121] developed an original method that involved using Ni phyllosilicates nanotubes as precursors to obtain, after H_2 treatment, small and well-dispersed nanoparticles (5-8 nm) of Ni^0 confined in the SiO_2 nanotubes with a porous shell having a thickness of 26.1 nm. The strong interaction with the support produced Ni nanoparticles that were resistant to the migration in the silica tubes, and consequently, to sintering. However, the dispersion estimated using H_2 chemisorption was quite low (3.7% for the highest one). The catalysts led to 81% and 78% conversions for CO_2 and CH_4, respectively, after 70 h at 700 °C under a relatively modest GHSV of 36 L g^{-1} h^{-1}.

Bian et al. (Table 3, entry 1) [116] also worked on a multicore-shell material with Mg as a promoter, which was synthesized successfully through the silica coating (thickness of 10 nm) of Ni-Mg phyllosilicate nanotubes (PSNTS). The authors reported that the thermal stability of the

catalyst was significantly improved due to the confinement of nickel and good interaction between Ni and the nanotubular support (core@tube confinement).

Despite the promising advances brought by the use of core-shell structures, the limitations of severe intra-bed and intra-particle heat transfer are nonetheless encountered with the Ni@oxide nanostructured catalysts that are implemented for the DRM process due to their poor thermal conductivity that generates cold-spots. According to the thermodynamic studies, cold spots not only decrease the reactor conversion, but they also facilitate carbon deposition, particularly on Ni-based catalysts. In this context, Chai and co-workers [122] (Table 3, entry 10) proposed the Ni@SiO_2/Al_2O_3/FeCrAl-fiber catalysts where the FeCrAl-alloy-based microfiber (referred to as FeCrAl-fiber) is an attractive material for the preparation of structured catalysts owing to its high temperature tolerance, mechanical robustness, high permeability, and particularly high heat transfer [124]. Ni@SiO_2/Al_2O_3/FeCrAl-fibers were prepared using a one-step, top-down, macro-micro-nano organization with the aid of cross-linking molecules, followed by a calcination treatment. The prepared fibers exhibited good activity (95% and 98% for CH_4 and CO_2 conversion, respectively, at 800 °C) and remained stable for 500 h due to their enhanced resistance to coke and Ni sintering resulting from their core-shell-like nanostructure. However, the reaction conditions tested were not so harsh (800 °C, GHSV = 5 L g^{-1} h^{-1}, CH_4/CO_2 = 1.0/1.1 (Table 3, entry 10) [122]).

Different structures have been obtained by following this strategy. However, it should be noted that in certain cases, this method may lead to a loss in the active sites due to the decreased accessibility of nickel. In addition, the synthesis of core-shell catalysts is difficult and the preparation methods are not so easy to implement. Moreover, only 10% of the reports involved GHSV values higher than 60 L g^{-1} h^{-1}. Evidently, this approach allows close control of the nature of the catalyst, which is of fundamental interest, although one may wonder regarding the applicability of such a synthesis approach in large-scale catalyst production. Therefore, metal deposition onto silica using conventional approaches, followed by coating with a porous silica layer, is perhaps a more practical solution in this regard.

5. Conclusion

Small Ni NPs confined in porous silica are capable of resisting against coke deposition and sintering by increasing the interactions with the support and/or exploiting the presence of physical barriers that reduce the migration of atoms and consequently their growth under harsh conditions. However, the conventional impregnation of porous silica is usually not sufficient to obtain the right materials. The key factor is the control of the interface between silica and nickel, which may rely heavily on the deposition method used. In the present review, several combinations of “nickel sources/support/impregnation methods” were discussed. Certain strategies beginning with original nickel precursors and/or implementing impregnations assisted by ligands or organic molecules appear to be complicated and are not always environment-friendly.

Therefore, it appears better to emphasize the use of the traditional deposition-precipitation method in combination with SBA-15 support [46], which generates a 10 wt.% catalyst that remains stable for 35 h under quite a high value of GHSV (240 L g^{-1} h^{-1}). One-pot approaches that incorporate nickel precursors in the synthesis gel of mesoporous supports, which are in the initial stages of development, could also be promising as they confer protection to nickel particles by a

porous silica coating. Combining Ni with promoters generates active and stable Ni-silica catalysts for DRM. The reasons for the improved stability of nickel vary with the nature of the promoter used. However, the addition of such species renders the preparation as well as the characterization of the catalysts further difficult. In addition, adding promoters may increase the cost of the catalysts. A simple comparison of Table 1 and Table 2 reveals that both the strategies (confinement and promoters) generate catalysts with good performances. However, just 8% of the reports concerning the use of promoters involved GHSV values higher than 100 L g^{-1} h^{-1}, while only 22% of the reports concerned the strategy of controlling the nickel particle size/confinement. In consideration of these remarks, it could be considered that the control of particle size and confinement might be more interesting provided that it is realized with an approach that is less complex and more feasible with industrial application.

The core-shell structure design is another approach that appears to be efficient for confining nickel nanoparticles in porous silica. The materials resulting from this approach appear to be quite interesting for DRM due to the possibility of nickel stabilization and the possibility of using different combinations with promoters.

Author Contributions

O. Daoura collected the data, wrote the paper. F. Launay and M. Boutros have initiated the project, helped O.D. for the structuration of the review and did various corrections.

Competing Interests

The authors have declared that no competing interests exist.

References

1. Ross JR, van Keulen AN, Hegarty ME, Seshan K. The catalytic conversion of natural gas to useful products. Catal Today. 1996; 30: 193-199.
2. Rani S, Padmanabhan E, Prusty BK. Review of gas adsorption in shales for enhanced methane recovery and CO_2 storage. J Pet Sci Eng. 2019; 175: 634-643.
3. Starr K, Gabarrell X, Villalba G, Talens L, Lombardi L. Life cycle assessment of biogas upgrading technologies. Waste Manage. 2012; 32: 991-999.
4. Talyan V, Dahiya RP, Anand S, Sreekrishnan TR. Quantification of methane emission from municipal solid waste disposal in Delhi. Resour Conserv Recy. 2007; 50: 240-259.
5. Todd RW, Cole NA, Casey KD, Hagevoort R, Auvermann BW. Methane emissions from southern High Plains dairy wastewater lagoons in the summer. Anim Feed Sci Technol. 2011; 166: 575-580.
6. Kumar N, Shojaee M, Spivey JJ. Catalytic bi-reforming of methane: From greenhouse gases to syngas. Curr Opin Chem Eng. 2015; 9: 8-15.
7. Aresta M, Dibenedetto A. Utilisation of CO_2 as a chemical feedstock: Opportunities and challenges. Dalton Trans. 2007; 2975-2992.
8. Arakawa H, Aresta M, Armor JN, Barteau MA, Beckman EJ, Bell AT, et al. Catalysis research of relevance to carbon management: Progress, challenges, and opportunities. Chem Rev. 2001; 101: 953-996.

9. Guo J, Hou Z, Gao J, Zheng X. Syngas production via combined oxy-CO_2 reforming of methane over Gd_2O_3-modified Ni/SiO_2 catalysts in a fluidized-bed reactor. Fuel. 2008; 87: 1348-1354.
10. Kawi S, Kathiraser Y, Ni J, Oemar U, Li Z, Saw ET. Progress in synthesis of highly active and stable nickel‑based catalysts for carbon dioxide reforming of methane. ChemSusChem. 2015; 8: 3556-3575.
11. Sivaiah MV, Petit S, Beaufort MF, Eyidi D, Barrault J, Batiot-Dupeyrat C, Valange S. Nickel based catalysts derived from hydrothermally synthesized 1:1 and 2:1 phyllosilicates as precursors for carbon dioxide reforming of methane. Microporous Mesoporous Mater. 2011; 140: 69-80.
12. Daoura O, Daher S, Kaydouh MN, El Hassan N, Massiani P, Launay F, Boutros M. Influence of the swelling agents of siliceous mesocellular foams on the performances of Ni-based methane dry reforming catalysts. Int J Hydrog Energy. 2018; 43: 17205-17215.
13. Balat M, Balat M, Kırtay E, Balat H. Main routes for the thermo-conversion of biomass into fuels and chemicals. Part 1: Pyrolysis systems. Energ Convers Manage. 2009; 50: 3147-3157.
14. Zhang X, Zhang Q, Tsubaki N, Tan Y, Han Y. Carbon dioxide reforming of methane over Ni nanoparticles incorporated into mesoporous amorphous ZrO_2 matrix. Fuel. 2015; 147: 243-252.
15. Wang C, Zhang Y, Wang Y, Zhao Y. Comparative studies of non-noble metal modified mesoporous M-Ni-CaO-ZrO_2 (M = Fe, Co, Cu) catalysts for simulated biogas dry reforming. Chin J Chem. 2017; 35: 113-120.
16. Daoura O, Kaydouh MN, El Hassan N, Massiani P, Launay F, Boutros M. Mesocellular silica foam-based Ni catalysts for dry reforming of CH_4 (by CO_2). J CO_2 Util. 2018; 24: 112-119.
17. Karaca H, Safonova OV, Chambrey S, Fongarland P, Roussel P, Griboval-Constant A, et al. Structure and catalytic performance of Pt-promoted alumina-supported cobalt catalysts under realistic conditions of Fischer–Tropsch synthesis. J Catal. 2011; 277: 14-26.
18. Khodakov AY, Chu W, Fongarland P. Advances in the development of novel cobalt Fischer−Tropsch catalysts for synthesis of long-chain hydrocarbons and clean fuels. Chem Rev. 2007; 107: 1692-1744.
19. Portugal UL, Santos AC, Damyanova S, Marques CM, Bueno JM. CO_2 reforming of CH_4 over Rh-containing catalysts. J Mol Catal A Chem. 2002; 184: 311-322.
20. Gheno SM, Damyanova S, Riguetto BA, Marques CM, Leite CA, Bueno JM. CO_2 reforming of CH_4 over Ru/zeolite catalysts modified with Ti. J Mol Catal A Chem. 2003; 198: 263-275.
21. Şener AN, Günay ME, Leba A, Yıldırım R. Statistical review of dry reforming of methane literature using decision tree and artificial neural network analysis. Catal Today. 2018; 299: 289-302.
22. Pakhare D, Spivey J. A review of dry (CO_2) reforming of methane over noble metal catalysts. Chem Soc Rev. 2014; 43: 7813-7837.
23. Aramouni NA, Touma JG, Tarboush BA, Zeaiter J, Ahmad MN. Catalyst design for dry reforming of methane: Analysis review. Renew Sust Energ Rev. 2018; 82: 2570-2585.
24. Arora S, Prasad R. An overview on dry reforming of methane: Strategies to reduce carbonaceous deactivation of catalysts. RSC Adv. 2016; 6: 108668-108688.
25. Nair MM, Kaliaguine S. Structured catalysts for dry reforming of methane. New J Chem. 2016; 40: 4049-4060.

26. Bian Z, Das S, Wai MH, Hongmanorom P, Kawi S. A review on bimetallic nickel‐based catalysts for CO_2 reforming of methane. ChemPhysChem. 2017; 18: 3117-3134.
27. Lavoie JM. Review on dry reforming of methane, a potentially more environmentally-friendly approach to the increasing natural gas exploitation. Front Chem. 2014; 2: 1-17.
28. Zhang Q, Long K, Wang J, Zhang T, Song Z, Lin Q. A novel promoting effect of chelating ligand on the dispersion of Ni species over Ni/SBA-15 catalyst for dry reforming of methane. Int J Hydrog Energy. 2017; 42: 14103-14114.
29. Zhang Q, Zhang T, Shi Y, Zhao B, Wang M, Liu Q, et al. A sintering and carbon-resistant Ni-SBA-15 catalyst prepared by solid-state grinding method for dry reforming of methane. J CO_2 Util. 2017; 17: 10-19.
30. Drobná H, Kout M, Sołtysek A, González-Delacruz VM, Caballero A, Čapek L. Analysis of Ni species formed on zeolites, mesoporous silica and alumina supports and their catalytic behavior in the dry reforming of methane. Reac Kinet Mech Cat. 2017; 121: 255-274.
31. Omoregbe O, Danh HT, Nguyen-Huy C, Setiabudi HD, Abidin SZ, Truong QD, et al. Syngas production from methane dry reforming over Ni/SBA-15 catalyst: Effect of operating parameters. Int J Hydrog Energy. 2017; 42: 11283-11294.
32. Gao XY, Ashok J, Widjaja S, Hidajat K, Kawi S. Ni/SiO_2 catalyst prepared via Ni-aliphatic amine complexation for dry reforming of methane: Effect of carbon chain number and amine concentration. Appl Catal A Gen. 2015; 503: 34-42.
33. Wen S, Liang M, Zou J, Wang S, Zhu X, Liu L, et al. Synthesis of a SiO_2 nanofibre confined Ni catalyst by electrospinning for the CO_2 reforming of methane. J Mater Chem A. 2015; 3: 13299-13307.
34. Wang M, Zhang Q, Zhang T, Wang Y, Wang J, Long K, et al. Facile one-pot synthesis of highly dispersed Ni nanoparticles embedded in HMS for dry reforming of methane. Chem Eng J. 2017; 313: 1370-1381.
35. Han JW, Parka JS, Choib MS, Lee H. Uncoupling the size and support effects of Ni catalysts for dry reforming of methane. Appl Catal B Environ. 2017; 203: 625-632.
36. Li H, He Y, Shen D, Cheng S, Wang J, Liu H, et al. Design an in-situ reduction of Ni/C–SiO_2 catalyst and new insights into pretreatment effect for CH_4–CO_2 reforming reaction. Int J Hydrog Energy. 2017; 42: 10844-10853.
37. Karam L, Casale S, El Zakhem H, El Hassan N. Tuning the properties of nickel nanoparticles inside SBA-15 mesopores for enhanced stability in methane reforming. J CO_2 Util. 2017; 17: 119-124.
38. Lovell EC, Fuller A, Scott J, Amal R. Enhancing Ni-SiO_2 catalysts for the carbon dioxide reforming of methane: Reduction-oxidation-reduction pre-treatment. Appl Catal B Environ. 2016; 199: 155-165.
39. Gao XY, Hidajat K, Kawi S. Facile synthesis of Ni/SiO_2 catalyst by sequential hydrogen/air treatment: A superior anti-coking catalyst for dry reforming of methane. J CO_2 Util. 2016; 15: 146-153.
40. Li W, Zhao Z, Guo X, Wang G. Employing a nickel‐containing supramolecular framework as Ni precursor for synthesizing robust supported Ni catalysts for dry reforming of methane. ChemCatChem. 2016; 8: 2939-2952.

41. Baktash E, Littlewood P, Pfrommer J, Schomacker R, Driess M, Thomas A. Controlled formation of nickel oxide nanoparticles on mesoporous silica using molecular Ni_4O_4 clusters as precursors: Enhanced catalytic performance for dry reforming of methane. ChemCatChem. 2015; 7: 1280-1284.
42. Gao XY, Liu H, Hidajat K, Kawi S. Anti‐coking Ni/SiO_2 catalyst for dry reforming of methane: Role of oleylamine/oleic acid organic pair. ChemCatChem. 2015; 7: 4188-4196.
43. Kang D, Lim HS, Lee JW. Enhanced catalytic activity of methane dry reforming by the confinement of Ni nanoparticles into mesoporous silica. Int J Hydrog Energy. 2017; 42: 11270-11282.
44. Yang W, He D. Role of poly(N-vinyl-2-pyrrolidone) in Ni dispersion for highly-dispersed Ni/SBA-15 catalyst and its catalytic performance in carbon dioxide reforming of methane. Appl Catal A Gen. 2016; 524: 94-104.
45. Kaydouh MN, El Hassan N, Davidson A, Casale S, El Zakhem H, Massiani P. Highly active and stable Ni/SBA-15 catalysts prepared by a “two solvents” method for dry reforming of methane. Microporous Mesoporous Mater. 2016; 220: 99-109.
46. Rodriguez-Gomez A, Pereñiguez R, Caballero A. Nickel particles selectively confined in the mesoporous channels of SBA-15 yielding a very stable catalyst for DRM reaction. J Phys Chem B. 2018; 122: 500-510.
47. Gálvez ME, Albarazi A, Da Costa P. Enhanced catalytic stability through non-conventional synthesis of Ni/SBA-15 for methane dry reforming at low temperatures. Appl Catal A Gen. 2015; 504: 143-150.
48. Tian J, Ma B, Bu S, Yuan Q, Zhao C. One-pot synthesis of highly sintering- and coking-resistant Ni nanoparticles encapsulated in dendritic mesoporous SiO_2 for methane dry reforming. Chem Commun. 2018; 54: 13993-13996.
49. Xu L, Zhang J, Wang F, Yuan K, Wang L, Wu K, et al. One-step synthesis of ordered mesoporous $CoAl_2O_4$ spinel-based metal oxides for CO_2 reforming of $CH4^+$. RSC Adv. 2015; 5: 48256-48268.
50. Xu L, Song H, Chou L. One-pot synthesis of ordered mesoporous NiO–CaO–Al_2O_3 composite oxides for catalyzing CO_2 reforming of CH_4. ACS Catal. 2012; 2: 1331-1342.
51. Kobylinski TP, Kibby CL, Pannell RB, Eddy EL. ROR-activated catalyst for synthesis gas conversion. Patent US4729981. 1986.
52. Unmuth EE, Schwartz LH, Butt JB. Iron alloy Fischer-Tropsch catalysts: I: Carburization studies of the Fe Ni system. J Catal. 1980; 63: 404-414.
53. Tang L, Yamaguchi D, Leita B, Sage V, Burke N, Chiang K. The effects of oxidation–reduction treatment on the structure and activity of cobalt-based catalysts. Catal Commun. 2015; 59: 166-169.
54. Yu T, Wu Z, Kim WS. Mild temperature synthesis of gold nanoplates using polyethyleneimine and their improved surface enhanced Raman signal. RSC Adv. 2014; 4: 37516-37521.
55. Shahzad A, Kim WS, Yu T. Synthesis, stabilization, growth behavior, and catalytic activity of highly concentrated silver nanoparticles using a multifunctional polymer in an aqueous-phase. RSC Adv. 2015; 5: 28652-28661.
56. Yu T, Kim R, Park H, Yi T, Kim WS. Mechanistic study of synthesis of gold nanoparticles using multi-functional polymer. Chem Phys Lett. 2014; 592: 265-271.

57. Van der meer J, Bardez-Giboire I, Mercier C, Revel B, Davidson A, Denoyel R. Mechanism of metal oxide nanoparticle loading in SBA-15 by the double solvent technique. J Phys Chem C. 2010; 114: 3507-3515.
58. J. W. Geus, Dutch pat. Appl. 6705,259, 1967: 6813,236, 1968.
59. Burattin P, Che M, Louis C. Molecular approach to the mechanism of deposition−precipitation of the Ni(II) phase on silica. J Phys Chem B. 1998; 102: 2722-2732.
60. Tanev PT, Pinnavaia TJ. A neutral templating route to mesoporous molecular sieves. Science. 1995; 267: 865-867.
61. Bian Z, Kawi S. Highly carbon-resistant Ni–Co/SiO_2 catalysts derived from phyllosilicates for dry reforming of methane. J CO_2 Util. 2017; 18: 345-352.
62. Xin J, Cui H, Cheng Z, Zhou Z. Bimetallic Ni-Co/SBA-15 catalysts prepared by urea co-precipitation for dry reforming of methane. Appl Catal A Gen. 2018; 554: 95-104.
63. Gao X, Tan Z, Hidajat K, Kawi S. Highly reactive Ni-Co/SiO_2 bimetallic catalyst via complexation with oleylamine/oleic acid organic pair for dry reforming of methane. Catal Today. 2017; 281: 250-258.
64. Erdogan B, Arbag H, Gazi NY. SBA-15 supported mesoporous Ni and Co catalysts with high coke resistance for dry reforming of methane. Int J Hydrog Energy. 2018; 43: 1396-1405.
65. Wu T, Zhang Q, Cai W, Zhang P, Song X, Sun Z, et al. Phyllosilicate evolved hierarchical Ni- and Cu–Ni/SiO_2 nanocomposites for methane dry reforming catalysis. Appl Catal A Gen. 2015; 503: 94-102.
66. Lovell EC, Horlyck J, Scott J, Amal R. Flame spray pyrolysis-designed silica/ceria-zirconia supports for the carbon dioxide reforming of methane. Appl Catal A Gen. 2017; 546: 47-57.
67. Zhao X, Lu M, Li H, Fang J, Shi L, Zhang D. In situ preparation of Ni nanoparticles in cerium-modified silica aerogels for coking- and sintering-resistant dry reforming of methane. New J Chem. 2017; 41: 4869-4878.
68. Zhao X, Li H, Zhang J, Shi L, Zhang D. Design and synthesis of NiCe@m-SiO_2 yolk-shell framework catalysts with improved coke- and sintering-resistance in dry reforming of methane. Int J Hydrog Energy. 2016; 41: 2447-2456.
69. Akri M, Chafik T, Granger P, Ayrault P, Batiot-Dupeyrat C. Novel nickel promoted illite clay based catalyst for autothermal dry reforming of methane. Fuel. 2016; 178: 139-147.
70. Albarazi A, Gálvez ME, Da Costa P. Synthesis strategies of ceria–zirconia doped Ni/SBA-15 catalysts for methane dry reforming. Catal Commun. 2015; 59: 108-112.
71. Xie T, Zhao X, Zhang J, Shi L, Zhang D. Ni nanoparticles immobilized Ce-modified mesoporous silica via a novel sublimation-deposition strategy for catalytic reforming of methane with carbon dioxide. Int J Hydrog Energy. 2015; 40: 9685-9695.
72. Kaydouh MN, El Hassan N, Davidson A, Casale S, El Zakhem H, Massiani P. Effect of the order of Ni and Ce addition in SBA-15 on the activity in dry reforming of methane. C R Chim. 2015; 18: 293-301.
73. Chen C, Wang X, Zhang L, Zou X, Ding W, Lu X. Synthesis of mesoporous Ni–La_2O_3/SiO_2 by ploy(ethylene glycol)-assisted sol-gel route as highly efficient catalysts for dry reforming of methane with a H_2/CO ratio of unity. Catal Commun. 2017; 94: 38-41.
74. Baudouin D, Margossian T, Rodemerck U, Webb PB, Veyre L, Krumeich F, et al. Origin of the improved performance in lanthanum‐doped silica‐supported Ni catalysts. ChemCatChem. 2017; 9: 586-596.

75. Oemar U, Kathiraser Y, Mo L, Ho XK, Kawi S. CO_2 reforming of methane over highly active La-promoted Ni supported on SBA-15 catalysts: Mechanism and kinetic modelling. Catal Sci Technol. 2016; 6: 1173-1186.
76. Omoregbe O, Danh HT, Abidin SZ, Setiabudi HD, Abdullah B, Vud KB, et al. Influence of lanthanide promoters on Ni/SBA-15 catalysts for syngas production by methane dry reforming. Procedia Eng. 2016; 148: 1388-1395.
77. Zhang L, Lian J, Li L, Peng C, Liu W, Xu X, et al. $LaNiO_3$ nanocube embedded in mesoporous silica for dry reforming of methane with enhanced coking resistance. Microporous Mesoporous Mater. 2018; 266: 189-197.
78. Taherian Z, Yousefpour M, Tajally M, Khoshandam B. A comparative study of ZrO_2, Y_2O_3 and Sm_2O_3 promoted Ni/SBA-15 catalysts for evaluation of CO_2/methane reforming performance. Int J Hydrog Energy. 2017; 42: 16408-16420.
79. Taherian Z, Yousefpour M, Tajally M, Khoshandam B. Catalytic performance of Samaria-promoted Ni and Co/SBA-15 catalysts for dry reforming of methane. Int J Hydrog Energy. 2017; 42: 24811-24822.
80. Taherian Z, Yousefpour M, Tajally M, Khoshandam B. Promotional effect of samarium on the activity and stability of Ni-SBA-15 catalysts in dry reforming of methane. Microporous Mesoporous Mater. 2017; 251: 9-18.
81. Chotirach M, Tungasmita S, Tungasmita DN, Tantayanon S. Titanium nitride promoted Ni-based SBA-15 catalyst for dry reforming of methane. Int J Hydrog Energy. 2018; 43: 21322-21332.
82. Sarkar B, Goyal R, Pendem C, Sasaki T, Bal R. Highly nanodispersed Gd-doped Ni/ZSM-5 catalyst for enhanced carbon-resistant dry reforming of methane. J Mol Catal A Chem. 2016; 424: 17-26.
83. Benrabaa R, Löfberg A, Caballero JG, Bordes-Richard E, Rubbens A, Vannier RN, et al. Sol–gel synthesis and characterization of silica supported nickel ferrite catalysts for dry reforming of methane. Catal Commun. 2015; 58: 127-131.
84. Al-Fatesh AS, Atia H, Abu-Dahrieh JK, Ibrahim AA, Eckelt R, Armbruster U, et al. Hydrogen production from CH_4 dry reforming over Sc promoted Ni / MCM-41. Int J Hydrog Energy. 2019; 44: 20770-20781.
85. Cao Y, Lu M, Fang J, Shi L, Zhang D. Hexagonal boron nitride supported mesoSiO_2-confined Ni catalysts for dry reforming of methane. Chem Commun. 2017; 53: 7549-7552.
86. Yao L, Shi J, Xu H, Shen W, Hu C. Low-temperature CO_2 reforming of methane on Zr-promoted Ni/SiO_2 catalyst. Fuel Process Technol. 2016; 144: 1-7.
87. Károlyi J, Németh M, Evangelisti C, Sáfrán G, Schay Z, Horváth A, et al. Carbon dioxide reforming of methane over Ni–In/SiO_2 catalyst without coke formation. J Ind Eng Chem. 2018; 58: 189-201.
88. Yao L, Wang Y, Shi J, Xu H, Shen W, Hu C. The influence of reduction temperature on the performance of ZrO_x/Ni-MnO_x/SiO_2 catalyst for low-temperature CO_2 reforming of methane. Catal Today. 2017; 281: 259-267.
89. Yao L, Shi J, Hu C. The structure, carbon deposition and stability of a ZrO_x/Ni–MnO_x/SiO_2 catalyst for the CO_2 reforming of methane. RSC Adv. 2015; 5: 90168-90177.
90. Littlewood P, Xie X, Bernicke M, Thomas A, Schomäcker R. $Ni_{0.05}Mn_{0.95}O$ catalysts for the dry reforming of methane. Catal Today. 2015; 242: 111-118.

91. Amin R, Liu B, Ullah S, Biao HZ. Study of coking and catalyst stability over CaO promoted Ni-based MCF synthesized by different methods for CH_4/CO_2 reforming reaction. Int J Hydrog Energy. 2017; 42: 21607-21616.
92. Zhang Q, Feng X, Liu J, Zhao L, Song X, Zhang P, et al. Hollow hierarchical Ni/MgO-SiO_2 catalyst with high activity, thermal stability and coking resistance for catalytic dry reforming of methane. Int J Hydrog Energy. 2018; 43: 11056-11068.
93. Nematollahi B, Rezaei M, Khajenoori M. Combined dry reforming and partial oxidation of methane to synthesis gas on noble metal catalysts. Int J Hydrog Energy. 2011; 36: 2969-2978.
94. Wang F, Xu L, Zhang J, Zhao Y, Li H, Li HX, et al. Tuning the metal-support interaction in catalysts for highly efficient methane dry reforming reaction. Appl Catal B Environ. 2016; 180: 511-520.
95. Wang HY, Au CT. Carbon dioxide reforming of methane to syngas over SiO_2-supported rhodium catalysts. Appl Catal A Gen. 1997; 155: 239-252.
96. Nagaoka K, Seshan K, Aika K, Lercher JA. Carbon deposition during carbon dioxide reforming of methane—comparison between Pt/Al_2O_3 and Pt/ZrO_2. J Catal. 2001; 197: 34-42.
97. Claridge JB, Green ML, Tsang SC. Methane conversion to synthesis gas by partial oxidation and dry reforming over rhenium catalysts. Catal Today. 1994; 21: 455-460.
98. Nurunnabi M, Mukainakano Y, Kado S, Miyazawa T, Okumura K, Miyao T, et al. Oxidative steam reforming of methane under atmospheric and pressurized conditions over Pd/NiO–MgO solid solution catalysts. Appl Catal A Gen. 2006; 308: 1-12.
99. Miyata T, Li D, Shiraga M, Shishido T, Oumi Y, Sano T, et al. Promoting effect of Rh, Pd and Pt noble metals to the Ni/Mg(Al)O catalysts for the DSS-like operation in CH_4 steam reforming. Appl Catal A Gen. 2006; 310: 97-104.
100. Li D, Shishido T, Oumi Y, Sano T, Takehira K. Self-activation and self-regenerative activity of trace Rh-doped Ni/Mg(Al)O catalysts in steam reforming of methane. Appl Catal A Gen. 2007; 332: 98-109.
101. Lucci FR, Marcinkowski MD, Lawton TJ, Sykes EC. H_2 activation and spillover on catalytically relevant Pt–Cu single atom alloys. J Phys Chem C. 2015; 119: 24351-24357.
102. Tanksale A, Beltramini JN, Dumesic JA, Lu GQ. Effect of Pt and Pd promoter on Ni supported catalysts—A TPR/TPO/TPD and microcalorimetry study. J Catal. 2008; 258: 366-377.
103. Damyanova S, Pawelec B, Arishtirova K, Fierro JL, Sener C, Dogu T. MCM-41 supported PdNi catalysts for dry reforming of methane. Appl Catal B Environ. 2009; 92: 250-261.
104. Pinheiro AN, Valentini A, Sasaki JM, Oliveira AC. Highly stable dealuminated zeolite support for the production of hydrogen by dry reforming of methane. Appl Catal A Gen. 2009; 355: 156-168.
105. Liu D, Cheo WN, Lim YW, Borgna A, Lau R, Yang Y. A comparative study on catalyst deactivation of nickel and cobalt incorporated MCM-41 catalysts modified by platinum in methane reforming with carbon dioxide. Catal Today. 2010; 154: 229-236.
106. de Miguel SR, Vilella IM, Maina SP, San Jose-Alonso D, Román-Martínez MC, Illán-Gómez MJ. Influence of Pt addition to Ni catalysts on the catalytic performance for long term dry reforming of methane. Appl Catal A Gen. 2012; 435-436: 10-18.
107. Hou T, Lei Y, Zhang S, Zhang J, Cai W. Ethanol dry reforming for syngas production over Ir/CeO_2 catalyst. J Rare Earths. 2015; 33: 42-45.

108. Greeley J, Mavrikakis M. Alloy catalysts designed from first principles. Nat Mater. 2004; 3: 810-815.
109. Niu J, Ran J, Ou Z, Du X, Wang R, Qi W, et al. CO_2 dissociation over Pt_xNi_{4-x} bimetallic clusters with and without hydrogen sources: A density functional theory study. J CO_2 Util. 2016; 16: 431-441.
110. Li L, Zhou L, Ould-Chikh S, Anjum DH, Kanoun MB, Scaranto J, et al. Controlled surface segregation leads to efficient coke‐resistant nickel/platinum bimetallic catalysts for the dry reforming of methane. ChemCatChem. 2015; 7: 819-829.
111. You XJ, Wang X, Ma YH, Liu JJ, Liu WM, Xu XL, et al. Ni–Co/Al_2O_3 bimetallic catalysts for CH_4 steam reforming: Elucidating the role of Co for improving coke resistance. ChemCatChem. 2014; 6: 3377-3386.
112. Xu JK, Zhou W, Li ZJ, Wang JH, Ma JX. Biogas reforming for hydrogen production over nickel and cobalt bimetallic catalysts. Int J Hydrog Energy. 2009; 34: 6646-6654.
113. Li LD, Anjum DH, Zhu HB, Saih Y, Laveille PV, D'souza L, et al. Synergetic effects leading to coke‐resistant NiCo bimetallic catalysts for dry reforming of methane. ChemCatChem. 2015; 7: 427-433.
114. Zhang JG, Wang H, Dalai AK. Development of stable bimetallic catalysts for carbon dioxide reforming of methane. J Catal. 2007; 249: 300-310.
115. Takanabe K, Nagaoka K, Nariai K, Aika K. Titania-supported cobalt and nickel bimetallic catalysts for carbon dioxide reforming of methane. J Catal. 2005; 232: 268-275.
116. Bian Z, Suryawinata IY, Kawi S. Highly carbon resistant multicore-shell catalyst derived from Ni-Mg phyllosilicate nanotubes@silica for dry reforming of methane. Appl Catal B Environ. 2016; 195: 1-8.
117. Zhang J, Li F. Coke-resistant Ni@SiO_2 catalyst for dry reforming of methane. Appl Catal B Environ. 2015; 176-177: 513-521.
118. Peng H, Zhang X, Zhang L, Rao C, Lian J, Liu W, et al. One-pot facile fabrication of multiple nickel nanoparticles confined in microporous silica giving a multiple-cores@shell structure as a highly efficient catalyst for methane dry reforming. ChemCatChem. 2017; 9: 127-136.
119. Wang C, Qiu Y, Zhang X, Zhang Y, Sun N, Zhao Y. Geometric design of a Ni@silica nano-capsule catalyst with superb methane dry reforming stability: Enhanced confinement effect over the nickel site anchoring inside a capsule shell with an appropriate inner cavity. Catal Sci Technol. 2018; 8: 4877-4890.
120. Bian Z, Kawi S. Sandwich‐like silica@Ni@silica multicore–shell catalyst for the low‐temperature dry reforming of methane: Confinement effect against carbon formation. ChemCatChem. 2018; 10: 320-328.
121. Li Z, Wang Z, Jiang B, Kawi S. Sintering resistant Ni nanoparticles exclusively confined within SiO_2 nanotubes for CH_4 dry reforming. Catal Sci Technol. 2018; 8: 3363-3371.
122. Chai R, Zhao G, Zhang Z, Chen P, Liu Y, Lu Y. High sintering-/coke-resistance Ni@SiO_2/Al_2O_3/FeCrAl-fiber catalyst for dry reforming of methane: One-step, macro-to-nano organization via cross-linking molecules. Catal Sci Technol. 2017; 7: 5500-5504.
123. Gawande MB, Goswami A, Asefa T, Guo H, Biradar AV, Peng DL, et al. Core-shell nanoparticles: Synthesis and applications in catalysis and electrocatalysis. Chem Soc Rev. 2015; 44: 7540-7590.

124. Wu P, Li X, Ji S, Lang B, Habimana F, Li C. Steam reforming of methane to hydrogen over Ni-based metal monolith catalysts. Catal Today. 2009; 146: 82-86.